As-Accepted Manuscript

P.R. Pandeya*, I. Black, S. Karlen, Y.-C. Tseng*, A.B. Downie, C. Heiss, P. Azadi, **R.R. Schendel**†. **2025**. Hempseed cell wall polysaccharides are dominated by linear xylans and cellulose: Comprehensive polysaccharide profiling of cell walls from ten cultivars of industrial hemp, *Cannabis sativa* L. *Carbohydr. Polym.*, 362:123635. (doi.org/10.1016/j.carbpol.2025.123635)

Hempseed cell wall polysaccharides are dominated by linear xylans and cellulose: Comprehensive structural profiling of ten cultivars of industrial hemp, *Cannabis sativa* L.

Prakash Raj Pandeya[1], Ian M. Black[2], Steven D. Karlen[3], Christian Heiss[2], Yen-Chang Tseng[1], A. Bruce Downie[4], Parastoo Azadi[2], Rachel R. Schendel[1*]

[1]Department of Animal and Food Sciences, University of Kentucky, Lexington, Kentucky 40546, USA

[2]Complex Carbohydrate Research Center, University of Georgia, Athens, Georgia 30602, USA

[3]Department of Energy, Great Lakes Bioenergy Research Center, Wisconsin Energy Institute, University of Wisconsin–Madison, Madison, Wisconsin 53726, USA

[4]Department of Horticulture, University of Kentucky, Lexington, Kentucky 40546-0312, USA

***Correspondance:**

Dr. Rachel R. Schendel

rachel.schendel@uky.edu

Abstract

Hempseed is a rich source of dietary fiber; however, there has been limited research on the variability of carbohydrate composition in hempseed cell walls. The primary aim of this study was to conduct a comprehensive chemical and structural analysis of the cell wall polysaccharides in ten hempseed cultivars. Water-soluble polysaccharides (WSP) and water-insoluble residues (WIR) were isolated and subsequently analyzed for their monosaccharide composition using HPAEC-PAD, glycosyl linkage analysis using GC-MS, and structural characterization via NMR spectroscopy. All hempseed cultivars contained a high proportion of insoluble fibers and smaller amounts of soluble polysaccharides. Glucose and xylose were the most abundant components of the WIR fractions, while the WSP fractions contained abundant amounts of galactose, galacturonic acid, arabinose, rhamnose, and mannose. The results of linkage and spectroscopic analysis were consistent with the compositional analysis, identifying cellulose and acetylated linear xylans as primary components of WIR, and arabinogalactans, rhamnogalacturonans, heteromannans, xyloglucans, and arabinan as predominant in WSP. Overall, the study revealed a comparable cell wall structure among the analyzed hemp seed varieties. The high fiber content of whole hempseed-based ingredients presents significant potential for food manufacturers seeking to develop products with enhanced dietary fiber content, offering both functional and nutritional benefits for consumers.

Keywords: monosaccharide composition, glycosyl linkage, fiber, lignin, hemicellulose, pectin

Introduction

Cannabis sativa L. has been utilized for thousands of years for its diverse range of industrial as well as medicinal uses. The non-drug varieties of *Cannabis*, defined as having a delta-9-tetrahydrocannabinol level of less than 0.3%, are categorized as hemp. Hempseeds are small oval-shaped grains that contain high amounts of dietary fibers, essential fatty acids, polyphenols, and proteins, all beneficial to a healthy human diet and have thus gained increasing attention (Callaway, 2004; Rodriguez-Leyva & Pierce, 2010). In addition to their nutritional composition, hempseed also contains bioactive compounds such as cannabidiol, which may lead to potential health benefits such as neuroprotection, antioxidant, and immune system regulatory effects (Kitamura et al., 2020; Leonard et al., 2020). Comprising more than 25% of dietary fiber (Agbana et al., 2024; Callaway, 2004), which is important for promoting digestive health, weight management, and blood sugar regulation (Slavin, 2005), hempseed exhibits the potential to regulate metabolic stresses and enhance gut health when incorporated into the diet.

Dietary fibers are predominantly located within the cell wall, a complex structure enveloping plant cells that assumes a pivotal role in plant growth, development, and defense mechanisms. Carbohydrates constitute the primary component of the cell wall, participating in functions such as cell structure, signaling, and energy storage (Carpita & Gibeaut, 1993; O'Neill et al., 2004). Approximately 90% of the dry weight of primary cell walls consists of polysaccharides, while in the context of lignified secondary cell walls, polysaccharides make up around 60% of the dry weight (Pettolino et al., 2012). Characteristic polysaccharides of dicotyledonous plant cell walls like hemp are cellulose; hemicellulose, including linear xylans, xyloglucans, and mannans; and pectins. Structurally, cellulose manifests as unbranched, elongated chains of glucosyl residues that are stacked into highly-ordered microfibrils, whereas hemicellulose and pectins are characterized by branching and structural complexity(Albersheim et al., 2010). Recent models of cell wall architecture suggest that cellulose microfibrils interact with unbranched regions of hemicelluloses via hydrogen bonding, creating an interconnected network of polysaccharides. Additionally, a gel-like matrix comprising pectin and other polysaccharides occupies the interstices between microfibrils through non-covalent interactions with cellulose (Cosgrove, 2018; Wang et al., 2015). In dicotyledonous plants, xyloglucans are the principal hemicellulose in the primary cell wall, whereas xylans dominate in the secondary cell wall (Scheller & Ulvskov, 2010). In contrast to the primary cell wall, the secondary cell wall also consists of lignin, which is a complex, water-insoluble phenolic polymer with a high molecular weight that enhances the rigidity and hydrophobic attributes of plant cell wall and facilitates mineral transport through vascular bundles. The lignin content of plant materials holds relevance for various agricultural and industrial sectors (Liu et al., 2018; Pettolino et al., 2012).

The importance of cell wall polysaccharides in human health has been widely studied. Collins et al. summarized the health benefits of noncellulosic cell wall polysaccharides of grains, highlighting their potential role in preventing various metabolic diseases (Collins et al., 2010). A key significance of noncellulosic cell wall polysaccharides is their function as a nutritional substrate for the microbial population in the large intestine. These polysaccharides offer distinct physiochemical and functional properties, such as viscosity, water-holding capacity, and nutrient binding, which can influence fermentability, nutrient bioavailability, and the composition of gut microbes during the fermentation process (Holscher, 2017). Microbial fermentation of these polysaccharides produces short-chain fatty acids, which are known for their diverse health-promoting effects, contributing to the reduction of the risk of widespread metabolic diseases, including cancers and cardiovascular diseases (Den Besten et al., 2013; Dodd et al., 2011; Kromhout et al., 1982). Importantly, the fermentation process and downstream biological effects are influenced by structural features of polysaccharides, such as monosaccharide composition and degree of branching (Miao et al., 2022; Yu et al., 2022). In addition, plant polysaccharides also exhibit various health-promoting and biological activities, including cardioprotective, lipid-lowering, anti-diabetic, and immunomodulatory effects, outside the context of fermentation (Aboughe-Angone et al., 2011; Liu et al., 2015). Hempseed cell wall polysaccharides have also demonstrated a protective role against chemically induced oxidative damages in *in vitro* and animal models (Wen et al., 2019; Xue et al., 2020).

Understanding the composition and structural characteristics of hempseed cell wall carbohydrates may thus provide valuable insights into the potential applications in food and industrial sectors. Recent studies have begun to explore the composition of hempseed cell walls. For example, Schultz et al. provided the monosaccharide profile of alcohol-insoluble fractions from the hull and heart parts of 20 hempseed cultivars (Schultz et al., 2020). Alonso-Esteban et al., compared eight hempseed cultivars, exploring soluble sugars in methanol-water extracts of both whole and dehulled hempseeds, and evaluated various biological activities (Alonso-Esteban et al., 2022). The physicochemical properties of water-soluble polysaccharides of hempseed were determined in a separate study, comparing outcomes with flaxseed polysaccharides (Julakanti et al., 2023). However, none of these studies provided complete polysaccharide profiling with glycosyl linkage analysis. Leonard et al. conducted compositional and linkage analysis of polysaccharides from hempseed hulls, but not whole hempseeds (Leonard et al., 2022). Our recent study provided a comprehensive analysis of the cell walls from whole hempseed, including the monosaccharide and glycosyl linkage composition, as well as lignin content (Agbana et al., 2024). However, this work was limited to a single commercial hempseed cultivar. Screening studies reporting variation in cell wall polysaccharide composition and structure across different variants have been published for various cereal crops, including *Triticum aestivum* (wheat), *Hordeum vulgare* (barley), *Secale cereale* (rye), and *Avena sativa* (oats) (Andersson et al., 2008; Gebruers et al., 2008; Nystrom et al., 2008; Shewry et al., 2008). Nevertheless, a

significant knowledge gap remains regarding the variation in the composition and structure of cell wall polysaccharides among different hempseed variants. This study aims to present a comprehensive and comparative analysis of polysaccharides in the cell walls of ten hempseed cultivars grown under standard conditions, namely NWG 2730, Enecterol, Yuma, Lara, Fedora 17, Henola, Orion 33, Futura 75, Futura 83, and USO 31. By elucidating the structural composition and variability of cell wall polysaccharides among these cultivars, we aim to provide the foundation for further research into the nutritional and functional properties of hempseed carbohydrates, ultimately contributing to the development of hempseed-based products with targeted quality and nutritional value.

Materials and Methods

Plant materials

Seeds of 10 different hemp cultivars namely, NWG 2730, Enecterol, Yuma, Lara, Fedora 17, Henola, Orion 33, Futura 75, Futura 83, and USO 31, were kindly provided by Dr. Robert Pearce from the University of Kentucky. Seeds were grown in the 2022 hemp variety trial plots managed at the University of Kentucky's Spindletop Farm research station (2951 Agronomy Rd, Lexington, KY) and harvested in September 2022. The origin and primary uses (fiber, grain, or dual-purpose) of the evaluated hemp cultivars are outlined in **Table 1**. The whole hemp seeds were obtained, and the dockage from the seeds was separated manually.

Table 1. Name, origin, and primary use of the hemp cultivars evaluated.

Hemp cultivars	Country of origin	Primary use
NWG 2730	USA	dual-purpose*
Enecterol	Italy	dual-purpose
Yuma	China	fiber
Lara	Ukraine	dual-purpose
Fedora 17	France	dual-purpose
Henola	Poland	grain
Orion 33	France	dual-purpose
Futura 75	France	fiber
Futura 83	France	dual-purpose
USO 31	Ukraine	grain

*Dual-purpose refers to the use of the cultivar for both grain and fiber purposes.

Chemicals and reagents

Sodium phosphate buffer was prepared using sodium phosphate monobasic (NaH_2PO_4) and sodium phosphate dibasic (Na_2HPO_4), which were obtained from VWR Chemicals (Ohio, USA). Ion-chromatography-grade sodium hydroxide (NaOH) solution, purchased from Fisher Chemicals (New Jersey, USA), and sodium acetate anhydrous (NaOAc), purchased from Millipore (Massachusetts, USA), were used to prepare eluents for HPAEC-PAD analysis. Thermostable α-amylase from *Bacillus* (500 U/mL) and amyloglucosidase from *Aspergillus niger* (260 U/mL) were purchased from Sigma-Aldrich (Missouri, USA) for destarching. Methanolic HCl (1.25 M), used for polysaccharide hydrolysis, and acetyl bromide and hydroxylamine hydrochloride, used for lignin quantification, were purchased from Sigma. A sugar mixture standard solution was prepared by combining L-(-) fucose (Thermo Scientific, Waltham, MA, USA), L-(+) rhamnose monohydrate (Alfa Aesar), L-arabinose (VWR Chemicals), D-(+)-galactose (Acros Organics), D-(+)-glucose (Acros Organics,), D-(+)-xylose (Tokyo Chemicals, Japan), D-mannose (Tokyo Chemicals), D-galacturonic acid (Alfa Aesar), and D-glucuronic acid (Alfa Aesar). Other chemicals used for various purposes such as dimethyl sulfoxide (DMSO), acetone, ethanol, trifluoroacetic acid (TFA), glacial acetic acid, and sulfuric acid (H_2SO_4) were obtained from VWR Chemicals. Chemicals used for linkage analysis were N-methylimidazole (Sigma), acetic anhydride (J.T. Baker), 1-ethyl-3-methylimidazolium acetate [Emim][Ac] (Ambeed), dimsyl potassium base (made in house using potassium hydride (Sigma) and dimethyl sulfoxide [DMSO] (Fluka)), dichloromethane [DCM] (VWR), and lithium aluminum deuteride [$LiAlD_4$] (Strem chemicals). Ethylenediaminetetraacetic acid [EDTA] (VWR), peracetic acid [PAA] (Sigma), and DMSO (VWR) were used to isolate acetylated xylans. GH10 *endo*-1,4-β-xylanases from *Cellvibrio japonicus*, used to perform enzymatic digestion of the isolated acetylated xylans, was purchased from Megazyme (Bray, County Wicklow, Ireland).

Moisture content determination and crude defatting

Cleaned hemp seeds were coarsely ground with a food processor and dried in a vacuum oven (model 5861, Napco, USA) at 80 °C with 71.11 kPa vacuum to constant weight (≈50 h). Weights of the hemp seeds before and after drying were taken to calculate the moisture content. After drying, coarsely-ground seeds were ground again with a coffee grinder and defatted using acetone. The samples were weighed, placed evenly over a Whatman filter paper No. 2 (W&R Balston Ltd.) in a porcelain funnel, and washed with acetone at a solid-to-solvent ratio of 1:4 (w/v). The samples were dried in a fume hood overnight and weighed to calculate crude fat content as wet basis. The defatted samples were then milled using a ball mill to < 0.5 mm and stored in an airtight container until destarching.

Isolation of hempseed non-starch polysaccharides

Destarching and preparation of water-soluble and insoluble non-starch polysaccharide fractions of hempseed cell walls were completed in triplicate following the method described by Bunzel et al. (Bunzel et al., 2001), with slight modifications. Briefly, for each replicate, 20 g of defatted powder was suspended in sodium phosphate buffer (0.08 M, pH 6.2, 200 mL), and heated with 1.5 mL of thermostable α-amylase for 20 min at 92 °C with continuous shaking at 95 rpm (flasks were additionally swirled every 5 min to break up any surface clumps). The suspension was subsequently cooled over ice, and the pH was adjusted to 4.5 using 0.5 M HCl. The suspension was further incubated with 750 uL of amyloglucosidase for 30 min in a 60 °C water bath with the flasks being swirled every 5 minutes. The warm suspension was then centrifuged for 10 min at 5400 × *g*. The residue was washed with warm water (60 °C) three times (1 × 150 mL, 2 × 100 mL), and the aqueous supernatant and washes were set aside for the subsequent isolation of water-soluble polysaccharides (WSP). The water-insoluble residue (WIR) was further washed three times (3 × 150 mL) each with ethanol and acetone, and the ethanol and acetone supernatants were discarded. Residual acetone was evaporated from the WIR in a fume hood overnight, followed by vacuum oven drying (70 °C, 24 h). To obtain WSP, the volume of the retained aqueous supernatants and washes was determined and four volumes of absolute ethanol were added. Polysaccharides were allowed to precipitate out of the resulting 80% ethanol solution at 4 °C overnight, followed by centrifugation (5400 × *g*, 10 min) at room temperature, successive washing with ethanol (1 × 100 mL, 2 × 50 mL) and acetone (1 × 100 mL, 2 × 50 mL), and drying in a vacuum oven (70 °C, 24 h). The dry weights of WSP and WIR were determined, and samples were stored in a desiccator until further use.

Lignin quantification

Lignin was quantified in the hemp seed samples with the acetyl bromide soluble lignin (ABSL) method described by Barnes and Anderson (Barnes & Anderson, 2017). Briefly, WIR was shaken overnight with 90% dimethyl sulfoxide (DMSO) and thoroughly washed with ethanol and acetone. The lignin contents were extracted using 25% acetyl bromide in glacial acetic acid by boiling at 50 °C for 2 h. Lastly, the reaction was stopped by adding an additional amount of glacial acetic acid and the clear supernatant was mixed with 1.5 N NaOH and 0.5 M hydroxylamine hydrochloride followed by the measurement of absorption at 280 nm against a blank using a UV-Vis spectrophotometer (UV-2700, Shimadzu, Japan). The content of ABSL was calculated by employing the universal extinction coefficient (23.077 g^{-1} L cm^{-1}) derived by Fukushima and Kerley (Fukushima & Kerley, 2011).

Saeman hydrolysis and monosaccharide profiling

The hydrolysis of cellulosic and hemicellulosic material from WIR samples was done under Saeman conditions (Saeman et al., 1945) following the method described by Schendel et al. (Schendel et al., 2015). Briefly, 100 mg of WIR was mixed with 12 M H_2SO_4 (1.5 mL) and allowed to stand on ice for 30 min with vigorous vortexing for 1 min in every 10 min. The samples were then allowed to stand for 2 h at room temperature with vortexing for 1 min in every 30 min. The samples were diluted with water to 1.6 M H_2SO_4 and heated at 100 °C for 3 h. After cooling to room temperature, the hydrolysates were filtered through a 0.22 μm PTFE syringe filter, and 5 mL of the hydrolysate was neutralized and brought up to 50 mL. The hydrolysates were stored in a -40 °C freezer until further analysis, using HPAEC-PAD to separate and detect released monomers. A stock solution of standard sugar mix containing fucose, rhamnose, arabinose, galactose, glucose, xylose, mannose, galacturonic acid, and glucuronic acid was prepared for the construction of an external calibration curve. The stock standard mix solution was diluted to achieve 1, 7, 13, 19, 25, 50, 75, 100, and 125 μM and assessed for linearity of detector response over that range using Chromeleon software (Thermo Scientific). The chromatographic parameters and HPAEC-PAD operational method are presented in **Supplementary Table S1** and **Table S2**, respectively. The peaks corresponding to each monosaccharide were integrated using Chromeleon software, and peak areas were fitted to quadratic calibration curves in OriginPro 2017 software.

Methanolysis and monosaccharide profiling

The acid-catalyzed depolymerization of non-cellulosic polysaccharides was achieved using the methanolysis procedure. Methanolysis was followed by TFA hydrolysis to remove methyl groups, enabling HPAEC analysis, and was performed as described by De Ruiter et al. (De Ruiter et al., 1992) with slight modifications. Briefly, 20-25 mg of the samples (WIR or WSP) were heated in a gas-tight, crimp-top glass vial (Chemglass Life Science) at 80 °C for 16 h with 2 mL of anhydrous 1.25 M methanolic HCl. After cooling, an aliquot (40 uL) of each hydrolysate was transferred into a new vial and evaporated to dryness in a centrifugal evaporator at 45 °C. The dried samples were then TFA hydrolyzed with 500 μL of 2 M TFA at 121 °C for 1 h. The hydrolysates were cooled and evaporated to dryness in a centrifugal evaporator at 45 °C, then remaining traces of TFA were removed by coevaporation with ethanol (2 × 200 μL). Finally, the dried residues were dissolved in 300 μL of water and filtered through a 0.22 μm PTFE syringe filter. The monosaccharide detection and quantification was performed using HPAEC-PAD as described above.

Linkage analysis (methylation)

Glycosyl linkage analysis was performed at the Complex Carbohydrate Research Center (CCRC), University of Georgia, by producing partially methylated alditol acetate (PMAA) derivatives from the samples (WIR and WSP), which were identified using gas chromatography-mass spectrometry (GC-MS). The procedure is a slight modification of the one described by Black et al. (Black et al., 2023). Briefly, the samples were acetylated using N-methylimidazole and acetic anhydride in the ionic liquid 1-ethyl-3-methylimidazolium acetate. The acetylated samples were dialyzed against DI water for 3 days in a 3-kDa MWCO dialysis membrane. The samples were then methylated using dimsyl potassium base. Following extraction into DCM, the carboxylic acid methyl esters were reduced using $LiAlD_4$ in THF (80 °C, 4 h). After a second dialysis as before, the samples were remethylated using two rounds of treatment with sodium hydroxide (15 min each) and methyl iodide (45 min each). The samples were then hydrolyzed using 2 M TFA (2 h in sealed tube at 120 °C), reduced with $NaBD_4$, and acetylated using acetic anhydride/TFA. The resulting PMAAs were analyzed on an Agilent 7890A GC interfaced to a 5975C MS (electron impact ionization mode); separation was performed on a 30 m Supelco SP-2330 bonded phase fused silica capillary column (30 m × 0.25 mm ID). The initial oven temperature was set at 60 °C, followed by a temperature ramp of 27.5 °C per minute until reaching 170 °C. The ramp rate was then reduced to 4 °C per minute until the temperature reached 235 °C, where it was held for 2 minutes. Subsequently, the temperature was ramped at 3 °C per minute until a final temperature of 240 °C was achieved, which was held for 8 min.

Isolation of acetylated xylans and endoxylanase digestion

Acetylated xylans were isolated from WIR following the protocol (mild delignification with peracetic acid followed by DMSO extraction) described by de Carvalho et al. (de Carvalho et al., 2017). Following isolation, the isolated material was lyophilized, and a sample (50 mg) was dissolved in DMSO-*d*6 and subjected to NMR analysis. Endoxylanase digestion of a portion of the isolated acetylated xylans was performed according to the method reported by Joyce et al. (Joyce et al., 2023). Following digestion, the enzymatic hydrolysate was also lyophilized, re-dissolved in DMSO-*d*6, and subjected to NMR analysis.

NMR analysis

The WIR fractions were prepared for solution-state NMR analysis through ball milling and swelling the milled material directly in DMSO-d_6 according to the protocol by Landucci et al. (Landucci et al., 2020). Each WIR sample (300 mg) was milled using a Fritsch Pulverisette 7 (Germany) in 20 mL agate-lined jars with 10 × 10 mm agate ball bearings at 600 rpm for a total duration of 4 h 10 min (interval: 5 min, break: 5 min, repeated 25 cycles). For NMR analysis, both the ball-milled WIR and WSP fractions (30–50 mg) were mixed with 600 µL of DMSO-d_6 in 5-mm NMR tubes, followed by sonication with occasional vortexing until a uniform gel was formed.

The 2D heteronuclear single-quantum coherence (HSQC) NMR experiments for WIR fractions were conducted at the Wisconsin Energy Institute on a Bruker Biospin (Billerica, MA) AVANCE NEO 700 MHz spectrometer, equipped with a 5-mm QCI $^{1}H/^{31}P/^{13}C/^{15}N$ cryoprobe, whereas experiments for WSP, acetylated xylans isolated from WIR, and oligosaccharides generated by endoxylanase digestion of the acetylated xylans were performed at the University of Kentucky on a Bruker AVANCE NEO 600 MHz high-performance digital NMR spectrometer with a triple resonance TXI cryoprobe. The central DMSO solvent peak served as the internal reference (δC 39.5, δH 2.49 ppm).

For the WIR gel-state samples, the HSQC experiments used the 'hsqcetgpsisp2.2' pulse sequence with acquisition parameters as follows: spectra were acquired from 12.32 to −0.66 ppm in F2 (^{1}H) with 1724 data points (acquisition time, 100 ms), and from 220 to −5 ppm in F1 (^{13}C) with 618 increments (F1 acquisition time, 8 ms) and 48 scans with a 1 s interscan delay. The d_{24} delay was set to 0.89 ms. A NOESY experiment was also performed on a representative WIR gel-state sample.

Similarly, for WSP fractions, isolated acetylated xylans, and acetylated xylooligosaccharides, HSQC experiments were performed in DMSO-d_6 using the 'hsqcedetgpsisp2.3' multiplicity-edited pulse sequence with the acquisition parameters as follows: from 19.83 to −0.66 ppm in F2 (^{1}H) with 2048 data points (acquisition time, 86 ms), and from 165 to −5 ppm in F1 (^{13}C) with 256 increments (F1 acquisition time, 5.1 ms) and 64 scans with a 1 s interscan delay. The d_{16} delay was set to 0.20 ms. Data processing utilized Bruker's Topspin 4.4.1 software, applying typical matched Gaussian apodization (GB = 0.001, LB = −0.5) in F2 and a squared cosine-bell function in F1 (without linear prediction). For acetylated xylans and acetylated xylooligosaccharides, HSQC-TOCSY, COSY, and HMBC experiments were also performed.

Anomeric and *O*-acetylated peaks from glycosyl residues in the WIR were identified by comparison with values reported in the literature (Brennan et al., 2012; Falk & Stanek, 1997; Golovchenko et al., 2024; Kim & Ralph, 2014; Lucyszyn et al., 2011; Rencoret et al., 2018; Shakhmatov et al., 2017; Teleman et al., 2000; Unda et al., 2017). Unequivocal confirmation of the *O*-acetylation pattern was achieved through NMR

analysis of acetylated xylooligosaccharides obtained from the enzymatic digestion of acetylated xylans isolated from the WIR fraction.

Statistical analysis

Statistical analyses were performed with OriginPro 2017 software using a one-way analysis of variance (ANOVA) followed by Tukey's means comparison tests. All data are presented as the mean ± standard deviation (SD) of triplicate analyses, unless otherwise specified. Statistical significance was assigned for experiment-wise p-values ≤ 0.05.

Results and Discussion

Moisture, crude fat, and cell wall material (insoluble and soluble) contents in hempseed cultivars

The moisture content, crude fat content, and yield of insoluble and water-soluble cell wall fractions from the analyzed hempseed cultivars are shown in **Figure 1**. The moisture content was comparable among the cultivars and ranged between 3.18 – 4.03% (**Figure 1A**), with the exception of Yuma, which had a significantly higher moisture content (7.25%). Our values are on the lower end of previously reported moisture contents in hempseed, but they still fall within the overall range of literature values (Alonso-Esteban et al., 2022; Callaway, 2004; House et al., 2010; Vonapartis et al., 2015), which vary from 1.1% (Vonapartis et al., 2015) to 9.2% (House et al., 2010). Another research group reported a moisture content of 5.7% for the Fedora 17 cultivar (Alonso-Esteban et al., 2022), which was higher than the moisture content of our sample (3.2%), but we did not find proximate data for the other nine cultivars in our portfolio. The crude fat contents in the whole hempseed cultivars in the present study range from 20.72% in Lara to 24.79% in Enecterol **(Figure 1B)**. Previous reports have shown slightly higher fat contents, ranging from 26.6% to 37.8%, in whole hemp seeds (Alonso-Esteban et al., 2022; Callaway, 2004; Schultz et al., 2020; Vonapartis et al., 2015).

The WSP and WIR cell wall materials were present at a ratio of approximately 1:10 in the analyzed hempseed cultivars. The contents of soluble and insoluble residues among all hempseed cultivars were comparable, ranging from 5.64 to 6.79% and 55.06 to 60.89%, respectively, of the dry weights of whole grains (**Figure 1C** and **1D**; values not corrected for protein and ash). This study utilized whole hemp seeds for analysis. Previous investigations have reported a higher fiber content in whole hemp seeds compared to

dehulled seeds (Zając et al., 2019), which is not surprising, given the high dietary fiber content of the hulls. Leonard et al. determined a total dietary fiber content of around 80% in hempseed hulls, summing from around 16% and 64% of water-soluble and insoluble fiber, respectively (Leonard et al., 2022). Other reports of total dietary fiber contents in whole hempseed range from 28-43% (Agbana et al., 2024; Callaway, 2004; Zając et al., 2019). Additionally, the hempseed fiber contents have also been determined using the acid detergent and neutral detergent fiber methods, which ranged from 22-30% and 28-40%, respectively (Alonso-Esteban et al., 2022; House et al., 2010; Vonapartis et al., 2015). Variations in fiber content among different studies can partially be attributed to the diversity in the employed experimental procedures, but nevertheless, it is clear that non-starch cell wall material makes up a substantial proportion of whole hempseeds.

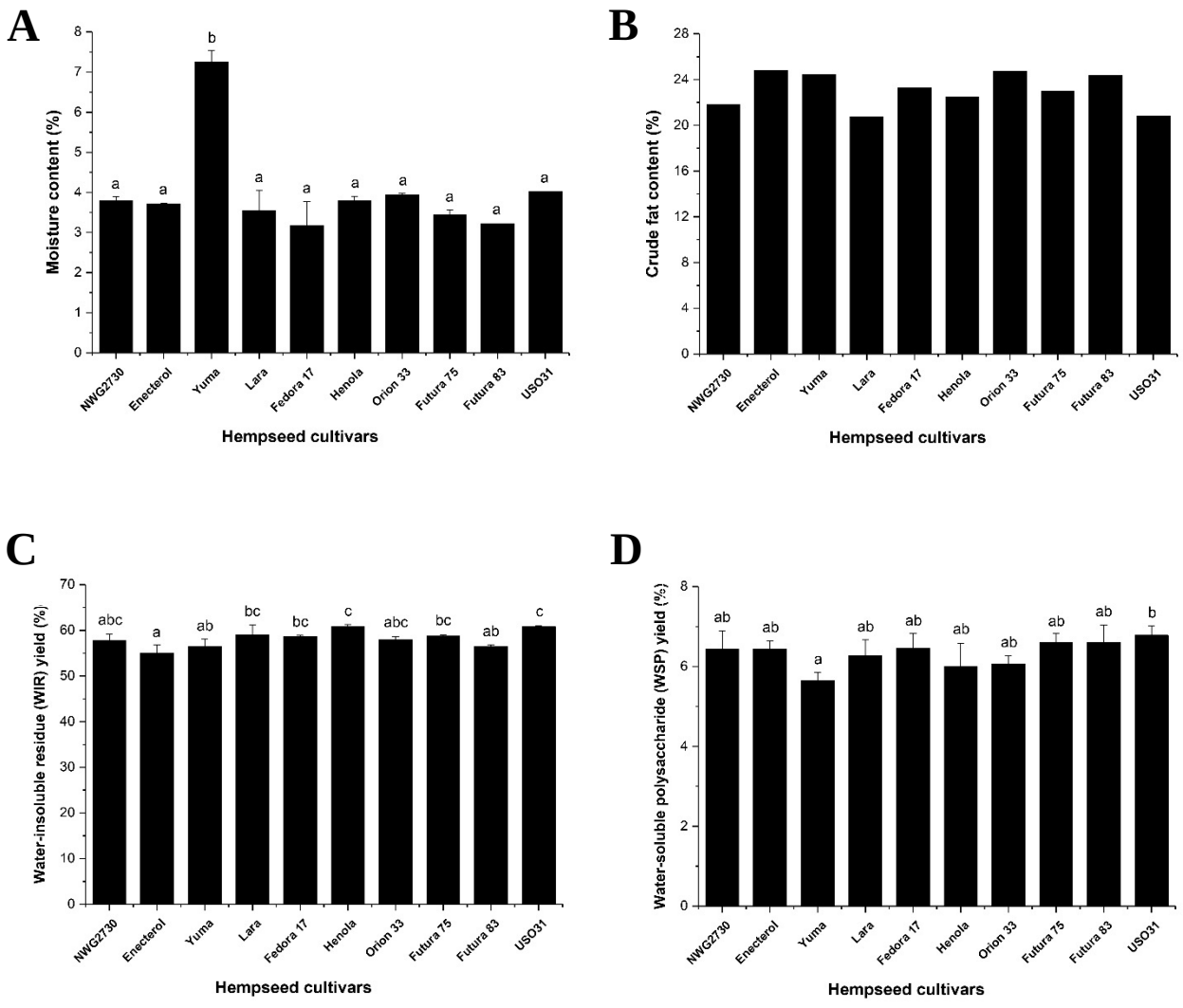

Figure 1. Moisture content (A), crude fat content (B), water-insoluble cell wall material yield (C), and water-soluble cell wall material yield (D) in ten hempseed cultivars. The moisture and crude fat contents are presented relative to the weight of whole wet hempseed, while the WIR and WSP yields are presented relative to the weight of whole dry hempseed. Statistical analysis was done using one-way ANOVA followed by Tukey's multiple comparison test. Results are presented as the mean ± standard deviation (n = 3), except fat content (n = 1). The assigned superscript letters show a level of significant differences among different cultivars. Note: The values are not corrected for protein and ash in insoluble and soluble polysaccharide materials.

Lignin content in hempseed cell walls

Lignin is one of the most abundant organic materials on earth (Chio et al., 2019). In terms of animal nutrition, a lower lignin content may be preferable for better digestibility. The lignin composition is inversely proportional to the effectiveness of converting plant carbohydrates into essential nutrition (Lacayo et al., 2013). Conversely, from a human health perspective, lignin may offer some potential benefits, including antioxidant, antitumor, antimicrobial, and immunomodulatory activities in addition to its capability to bind bile acids and toxins in the gastrointestinal tract (Hamauzu & Mizuno, 2011; Martínez et al., 2012). Therefore, the ABSL lignin content was determined in the different variants of hempseeds. The lignin content in defatted hempseed cultivars ranged from 8.41 ± 2.17% in Lara to 12.50 ± 3.58% in Henola cultivars (**Figure 2**). In general, our results align with a previous study on 10 hempseed cultivars, reporting lignin contents ranging from 10.5% to 11.8% (Vonapartis et al., 2015). Another study conducted on 20 hempseed cultivars showed a slightly higher level of lignin, ranging from 16.0% to 19.5% (Schultz et al., 2020). The elevated lignin content reported in that study might be attributed to their analysis focusing on the hempseed hull. Schultz et al. used phloroglucinol red staining to show that lignin was mostly concentrated in the hulls, with only a trace observed in the heart (Schultz et al., 2020). Our previous study conducted in a single commercial whole hempseed variant showed 17% of ABSL lignin (Agbana et al., 2024), which was slightly higher than the present study.

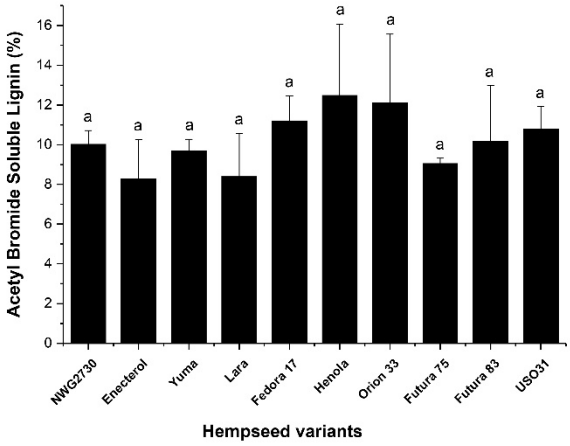

Figure 2. Acetyl bromide soluble lignin (ABSL) composition in ten hemp grain cultivars. Statistical analysis was done using one-way ANOVA followed by Tukey's multiple comparison test. Results are presented as the mean ± standard deviation (n = 3).

Monosaccharide composition of the hempseed cell wall materials

The monosaccharide compositions of hempseed cell wall materials were determined using two complimentary hydrolysis techniques. Before hydrolysis, the defatted hempseed samples underwent destarching through digestion with α-amylase and amyloglucosidase to reduce glucose originating from starch. The destarched residues contain null to 0.82% of residual starch after enzymatic digestion (data not shown). To capture water-soluble non-starch polysaccharides which were solubilized during destarching procedure, the WSP fractions were precipitated, collected, and subsequently analyzed separately. The water-insoluble residue (WIR) was expected to have a high cellulose content and was thus subjected to hydrolysis using the Saeman procedure. Here, strong sulfuric acid is used to achieve complete hydrolysis of glycosidic bonds in crystalline cellulose, but uronic acids are underestimated (De Ruiter et al., 1992; Liu et al., 2021). To capture glycosidic linkages involving uronic acids in the sample, methanolysis combined with TFA hydrolysis was performed. Methanolysis, the first step of this procedure, cleaves glycosidic linkages and forms methyl glycosides, and subsequent TFA hydrolysis removes the methyl group, resulting in a single peak for each monosaccharide in HPAEC (De Ruiter et al., 1992). Anion exchange chromatography is an effective tool for the separation of the monosaccharides in the hydrolysates, since carbohydrates act as weak acids, and are transformed into oxyanions with high-pH eluents and are readily separated using anion-exchange columns (Corradini et al., 2012). The well-separated HPAEC chromatograms for external standards and hydrolyzed hempseed samples are illustrated in **Supplementary Chromatograms 1 to 4**.

Monosaccharide compositions of WIR and WSP of hempseed cultivars achieved through the complementary hydrolysis procedures are shown in **Figure 3**. The hempseed cell wall polysaccharides of each cultivar are comprised of at least nine monosaccharides, including fucose, rhamnose, arabinose, galactose, glucose, xylose, mannose, galacturonic acid, and glucuronic acid. The compositions are consistent with our previous study (Agbana et al., 2024). Wen et al. similarly identified these nine monosaccharides in water-soluble polysaccharide fractions of hempseed (Wen et al., 2019). A comparison of the molar ratios of individual monosaccharides released from both hydrolysis procedures among the hempseed cultivars is presented in **Supplementary Figures S1 to S3**. Statistically, the quantity of each monosaccharide was comparable among the hempseed cultivars.

The Saeman hydrolysis of WIR samples of each hempseed cultivar showed a predominance of glucose (49.29-52.03%) and xylose (39.40-42.37%), indicating cellulose and xylans were abundant in the WIR **(Figure 3A)**. Methanolysis of the same samples showed xylose (74.95-79.94%) as the predominant sugar, confirming the presence of a high amount of xylan in the sample **(Figure 3B)**. Glucuronic acid, which is a backbone substituent of acidic xylans, was also present. These results align with our prior findings analyzed in a single commercial hemp sample (Agbana et al., 2024). Consistent with our observations, methanolysis results from a previous study demonstrated a predominance of xylose (98.75-99.65%) in hempseed hulls (Leonard et al., 2022). Similarly, a separate study revealed xylose as a predominant monosaccharide in the non-cellulosic fractions of hulls of 20 hempseed variants (Schultz et al., 2020). The observation of a substantially lower proportion of glucose in the methanolysis hydrolysates compared to the Saeman hydrolysates arises because glucose from cellulose is not included in the methanolysis hydrolysates. Both hydrolysis procedures with the WIR fractions revealed comparable glucose contents among the studied cultivars whereas xylose contents are significantly higher in Henola and Orion 33 **(Supplementary Figure S1)**.

Because cellulose is water-insoluble, the WSP fractions were not subjected to the Saeman hydrolysis. Methanolysis of WSP samples revealed a predominant amount of galactose (25.11-29.32%), followed by mannose (14.3-20.07%), arabinose (11.17-16.43%), glucose (8.28-11.67%), galacturonic acid (7.26-10.76%), xylose (6.60-8.63%), and rhamnose (5.69-7.14%) **(Figure 3C)**. This result indicated the presence of abundant pectic rhamnogalacturonans with arabinan- and galactan-side chains, and arabinogalactans, along with a significant amount of xyloglucans and heteromannans in the WSP samples. In contrast, in our previous methanolysis results from a single commercial sample of whole hempseed, xylose was the most abundant monosaccharide in WSP, followed by galactose, arabinose, galacturonic acid, and mannose (Agbana et al., 2024). The rhamnose, arabinose, and glucose levels in WSP fractions varied across the studied cultivars, while the levels of other sugars were relatively consistent. Rhamnose was significantly

higher in USO31 and Lara, whereas arabinose and glucose were most abundant in Enecterol and Yuma cultivars, respectively **(Supplementary Figure S3)**. Collectively, the present study unveiled that the WSP comprised 81-86% non-acidic sugars, with the highest proportion observed in Yuma and Lara, and 14-19% acidic sugars, with the highest level in Henola and USO31 cultivars. A prior investigation, employing a colorimetric method for sugar content determination, reported that the water-soluble polysaccharides from hempseed contained 53% total sugars and 33% uronic acids, calculated using glucose and galacturonic acid, respectively, as the standards (Julakanti et al., 2023).

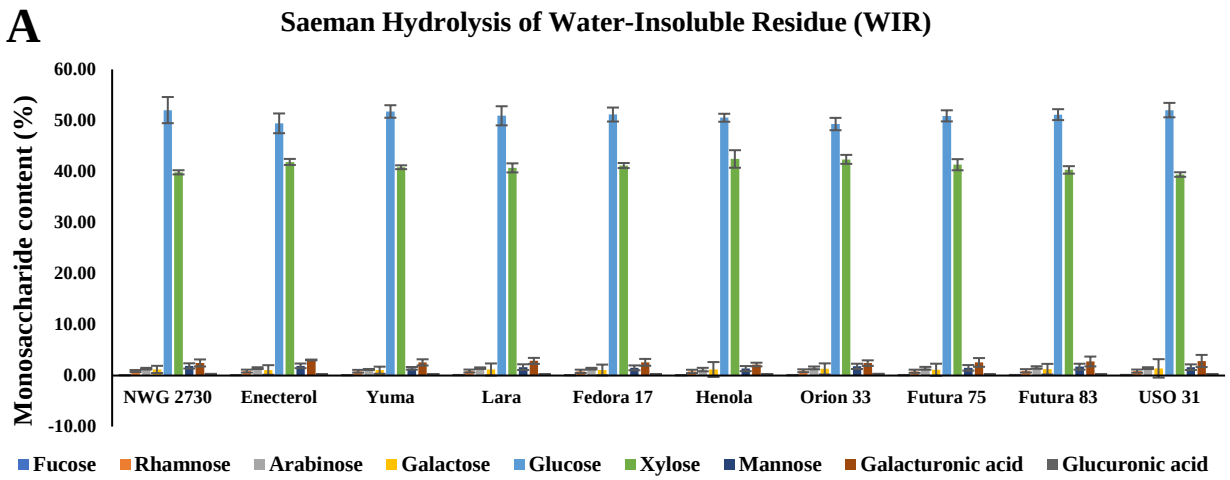

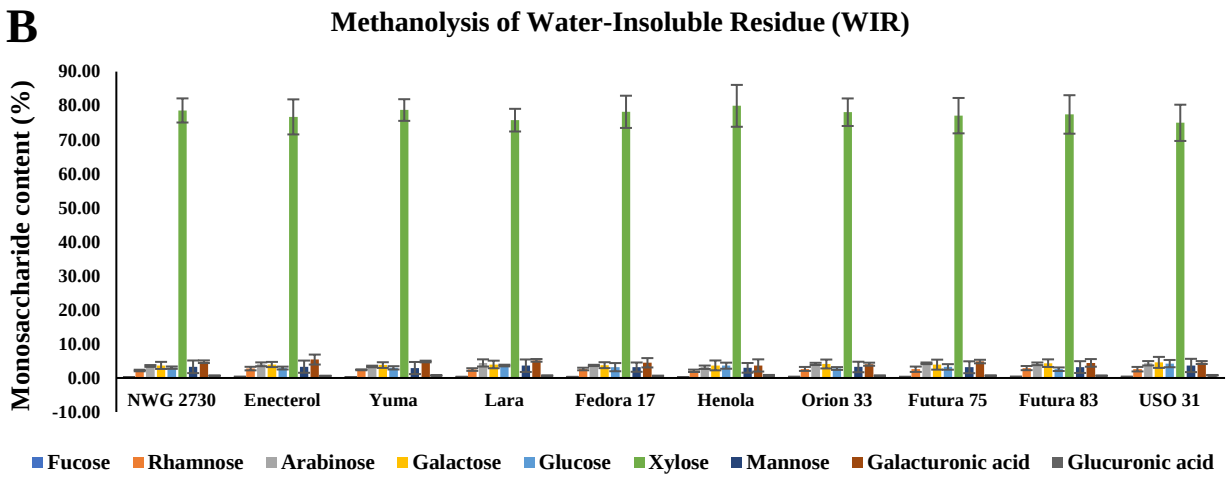

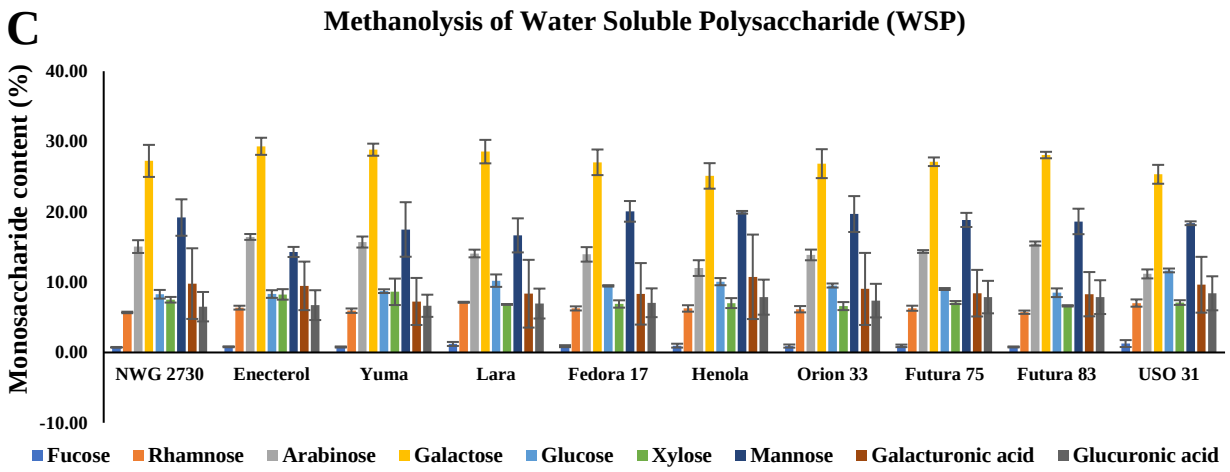

Figure 3. Molar concentration (%) of monosaccharides released from Saeman hydrolysis (A) and methanolysis (B) of water-insoluble residue, and from the methanolysis of water-soluble polysaccharide (C) fraction of hempseed cell walls. Results are presented as the mean ± standard deviation (n = 3).

Glycosyl linkage composition in hempseed cell wall polysaccharides

Further structural insights into the polysaccharides from the hempseed cell walls were obtained through methylation analysis of both WIR and WSP samples. The representative total ion chromatograms of the analyzed samples are shown in **Supplementary Chromatograms 5 to 24**. The possible glycosyl linkages associated with WIR and WSP are presented in **Table 2** and **Table 4**, respectively. Overall, our observations revealed a consistent alignment between our monosaccharide composition and linkage analysis results. Linkage analysis of the WIR samples showed them to be largely consistent among the different hempseed cultivars, with 4-Xyl*p* and 4-Glc*p* being the most abundant linkages **(Table 2)**. This confirms the results already indicated by the monosaccharide composition of the insoluble samples: whole hempseeds contain mostly cellulose and xylan in their cell walls. Several other linkages in smaller amounts can also be seen, representing different cell wall polysaccharide components that are present in the WIR samples in much lower amounts **(Table 2)**. The linkage analysis of WIR showed high levels of 2,3,4-Xyl*p*. The presence of t-Glc*p*A indicates the existence of acidic xylans substituted at *O*-3 and/or *O*-2 with glucuronic or 4-*O*-methyl-glucuronic acid, meaning that a portion of the 2,3,4-Xyl*p* residues could be legitimate, but numerically, this could not account for all of the 2,3,4-Xyl*p*, indicating some undermethylation. Repeating the linkage analysis following ball milling of the samples and incorporating additional methylation steps reduced, but did not fully eliminate the 2,3,4-Xyl*p*.

Assuming the 2,3,4-Xyl*p* was either undermethylated 4-linked xylose or legitimately di-substituted xylose, we may aggregate these xylose residues together with the less abundant 2,4-Xyl*p* and 3,4-Xyl*p* residues to roughly estimate the molar proportion of xylan in the samples **(Table 3)**. Terminal xylopyranose (t-Xyl*p*) is also assigned to xyloglucans and pectic xylogalacturonans and thus is not included in this estimate. Though xylans substituted with arabinose, e.g. arabinoxylans, are mostly prevalent in monocots, it is also possible that some of the t-Ara*f* in this study could arise from small amounts of arabinoxylan in the hempseed samples (Pettolino et al., 2012). Analogous to the assumptions regarding xylans, if 4-Glc*p* and terminal glucose are assigned to cellulose, we may approximate the proportion of cellulose in each sample. The approximate xylan proportion is remarkably consistent across the 10 hemp cultivars, ranging from ≈40% in Enecterol and USO 31 to 47% in Fedora, whereas the cellulose estimate ranged from ≈35% in Lara and USO 31 to 48% in Futura 75 **(Table 3)**. Statistically, all the analyzed hempseed cultivars contained comparable amounts of xylan and cellulose, respectively in their cell walls. Additionally, these values must be treated as approximates, since the presence of small amounts of 4,6-Glc*p* and t-Xyl*p* indicates the presence of low levels of insoluble xyloglucans in the WIR samples, meaning that a small portion of 4-Glc*p* actually belongs to xyloglucan, not cellulose. However, considering our monosaccharide analysis results **(Figure 3A-B)**, where a drastic decrease in molar glucose proportions was observed between the Saeman hydrolysates, which includes both cellulose and hemicellulose, and methanolysis hydrolysates, which does not include cellulose, the xyloglucan levels are clearly low and only slightly inflate the cellulose estimate. The key insight from these data is that the water-insoluble cell wall material of hempseeds from a variety of genetic backgrounds are predominantly composed of cellulose and xylan. These results are consistent with our previous investigation, which also demonstrated dominant amounts of xylan- and cellulose-related linkages in the water-insoluble fraction of a commercial whole hempseed (Agbana et al., 2024). Leonard et al. showed a predominance of 4-Glc*p* (35.5-53.5%) compared to 4-Xyl*p* (17.9-26.9%) in hempseed hulls, indicating a higher prevalence of cellulose than xylan (Leonard et al., 2022). In contrast, the comparatively higher recovery of xylose residues observed in our results from whole hempseed suggests that hempseed hearts are rich in xylose-bearing polysaccharides like xylans or xyloglucans. When compared to other dicot seeds, hempseed cell wall material has a notably higher xylan content. For example, a recent study reporting linkage analysis results from three varieties of destarched whole *Lupinus spp.* (lupin) seeds and lupin hulls recovered the 4-linked Xyl*p* residue at 3.5-9.3% and 24-30% of the total PMAAs, respectively (Keller et al., 2022). Lower abundances of 4-Xyl*p* in other dicot seeds are also reported, such as ≈2% in dehulled, destarched *Fagopyrum esculentum* (buckwheat) grain (Wefers & Bunzel, 2015), ≈2% in destarched *Chenopodium quinoa* (quinoa) grain (Wefers, Gmeiner, et al., 2015), and ≈3% in both destarched *Amarantus spp.* (amaranth) grain (Wefers, Tyl, et al., 2015) and destarched *Glycine max* (soybean) extraction meal (Wefers & Bunzel, 2016).

The water-soluble cell wall material of dicots may contain various polysaccharides, including pectins, xyloglucans, and heteromannans. The pectic polysaccharides within water-soluble fraction belong to structural classes such as homogalacturonan (HG), rhamnogalacturonan type I (RG-I), rhamnogalacturonan type II (RG-II), and xylogalacturonan. Additionally, water-soluble polysaccharides may include arabinogalactan type I (AG-I) and arabinogalactan type II (AG-II) (Chawla & Patil, 2010; Navarro et al., 2019; Ridley et al., 2001). The glycosyl residues obtained through linkage analysis of WSP fractions of hempseed fibers are presented in **Table 4**. Notably, the proportions of glycosyl linkages remain relatively consistent across the analyzed hempseed cultivars. The compositional analysis revealed galactose, mannose, and arabinose as the most abundant monosaccharides in the soluble fraction of hempseed **(Figure 3C)**. Linkage analysis further showed that the sample was predominantly composed of 3,6-Gal*p*, primarily derived from AG-II (Pettolino et al., 2022). The substantial recovery of 3-Gal*p*, 6-Gal*p*, t-Ara*f*, t-Gal*p*, and t-Rha*p* in the linkage analysis reinforced the prevalence of AG-II as the most abundant polysaccharide in the soluble fraction. These AG-II-associated residues were most prevalent in the Fedora 17 cultivar (~31%) and least in the Henola cultivar (~23%) **(Table 4)**.

Another abundant monosaccharide recovered from methanolysis compositional analysis is galacturonic acid (GalA) **(Figure 3C)**, and the associated residues with GalA recovered from linkage analysis include 4-Gal*p*A, 3,4-Gal*p*A, and t-Gal*p*A, indicative of pectic polysaccharides. 4-Gal*p*A is a core backbone component of all pectic polysaccharides, including homogalacturonan, RG-I, RG-II, and xylogalacturonan (Pettolino et al., 2012). The recovery of 3'-Api*f* confirmed the presence of RG-II. Furthermore, the detection of 3,4-Gal*p*A strongly suggests the presence of xylogalacturonan in hempseeds, which is a pectic polysaccharide commonly found in reproductive plant tissues (Ridley et al., 2001). The recovery of 2-Rha*p* and 2,4-Rha*p* and other associated linkages such as t-Ara*f*, t-Gal*p*, 5-Ara*f*, and 2,5-Ara*f*, underline the existence of RG-I with branched arabinan side chains in the WSP samples (Albersheim et al., 2010; Navarro et al., 2019; Pettolino et al., 2012). Lastly, the occurrence of 4-Gal*p* indicated the presence of linear galactan RG-I branches or AG-I.

The methanolysis compositional analysis also revealed a high content of mannose in the water-soluble sample, with Fedora 17 exhibiting the highest level among all cultivars **(Figure 3C)**. The plant cell wall polysaccharides associated with mannose are heteromannans, which function as storage polysaccharide as well as an energy resource for seed germination (Albersheim et al., 2010). Heteromannans manifest in four primary types: linear mannan, glucomannan, galactomannan, and galactoglucomannan (Singh et al., 2018). Galactomannan and galactoglucomannan, characterized by a β-(1→4)-linked-mannan backbone, are water-soluble branched types (Joseleau & Pérez, 2016). The abundant recovery of 4-Man*p* in our study suggested the presence of some unbranched (1-4)-β-mannan backbone regions, both in the WIR and WSP. In addition,

abundant t-Man*p* indicated the presence of short-chain mannans. As linear mannan is not readily soluble in water, the presence of more branching mannans in the WSP was expected. However, no 4,6-Man*p*, which is characteristic of the branched galactomannans and galactoglucomannans, was recovered in the WSP. Several unusual mannose residues, including 2-Man*p*, 2,3-Man*p*, and 2,6-Man*p*, were detected in the WSP fraction, which indicated a possibility of a 2-linked mannan backbone with *O*-3 and *O*-6 associated side-chain structures. However, these linkages have not been reported in plant mannans. The linkage analysis showed the Orion 33 and USO 31 contained the highest levels of mannose residues **(Table 3)**.

The 4-Glc*p* in the water-soluble material can arise both from xyloglucan and heteromannans, including glucomannan and galactoglucomannan. However, as discussed above, we did not find evidence of galactoglucomannans in the WSP. When considering glucomannans, it is generally observed that the ratio of mannose is consistently higher than glucose for these polysaccharides (Alonso-Sande et al., 2009). In this study, the amount of 4-Glc*p* is significantly higher than that of 4-Man*p* **(Table 4)**, indicating that 4-Glc*p* is also arising from other soluble polysaccharides, such as xyloglucan. The existence of soluble xyloglucans was confirmed by the presence of 4,6-Glc*p*, and the identification of 2-Xyl*p*, t-Xyl*p*, and t-Fuc*p* suggesting the F-motif xyloglucan branching pattern. The xyloglucan-associated linkages were found to be statistically comparable among all studied hempseed cultivars. The recovery of a small amount of 4-Xyl*p* showed that some linear xylans were present in the soluble samples, as well. Mixed linked β-glucans (MLG) are water-soluble in nature due to their possession of two types of linkages, preventing the compact folding of β-glucan chains (Chawla & Patil, 2010). So far, MLG has not been considered to be present in the cell wall of dicot plants (Holscher, 2017; Schendel et al., 2015). However, the presence of 3-Glc*p* together with 3,4-Glc*p* hints at the possibility of MLG in the hempseed cell walls, although definite confirmation would require additional analyses such as isolation, concentration, and NMR characterization of the purified sample.

Table 2. Major glycosyl linkages (% peak area) of the polysaccharides of WIR fraction deduced from identified partially methylated alditol acetates (PMAAs). Results are presented as the mean and standard deviation (SD) (n=3).

Glycosyl linkages	**Hempseed Cultivars- Water-Insoluble Polysaccharides (Area %)**									
	NWG 2730	**Enecterol**	**Yuma**	**Lara**	**Fedora 17**	**Henola**	**Orion 33**	**Futura 75**	**Futura 83**	**USO 31**
Glc*p* t-	0.86[a]	2.02[a]	1.38[a]	1.11[a]	1.39[a]	1.28[a]	1.44[a]	1.04[a]	1.29[a]	1.85[a]
SD	0.10	1.55	0.63	0.25	0.51	0.10	0.24	0.47	0.07	0.34

	3-	0.24[a]	0.72[ab]	0.37[a]	0.51[a]	0.51[a]	0.64[a]	0.47[a]	0.27[a]	0.38[a]	1.44[b]
	SD	0.10	0.26	0.15	0.23	0.13	0.11	0.17	0.00	0.16	0.73
	4-	45.94[a]	36.34[a]	41.67[a]	41.05[a]	33.96[a]	38.28[a]	42.00[a]	47.23[a]	45.37[a]	33.29[a]
	SD	4.95	2.65	0.88	8.64	4.73	5.63	3.18	6.23	4.96	4.78
	3,4-	0.85[a]	0.98[a]	0.69[a]	0.74[a]	0.86[a]	0.84[a]	0.51[a]	0.62[a]	0.59[a]	0.99[a]
	SD	0.17	0.22	0.17	0.12	0.11	0.32	0.10	0.22	0.23	0.36
	4,6-	1.72[ab]	3.28[ab]	1.84[ab]	2.31[ab]	1.31[a]	1.87[ab]	2.56[ab]	1.53[ab]	1.44[ab]	3.92[b]
	SD	0.46	1.17	0.15	0.48	0.87	0.85	0.56	0.63	0.95	1.75
	ΣGlc*p*	**49.61**	**43.34**	**45.95**	**45.72**	**38.02**	**42.90**	**46.97**	**50.70**	**49.07**	**41.48**
Xyl*p*	t-	0.46[a]	1.75[ab]	1.36[ab]	0.80[a]	1.57[ab]	1.24[ab]	1.71[ab]	0.99[ab]	1.30[ab]	2.19[b]
	SD	0.14	0.76	0.23	0.60	0.49	0.07	0.36	0.63	0.30	0.58
	4-	30.86[a]	27.40[a]	32.69[a]	28.72[a]	26.93[a]	29.64[a]	34.56[a]	32.50[a]	33.97[a]	27.18[a]
	SD	4.68	2.30	5.09	5.64	4.40	6.78	1.34	3.96	3.16	5.55
	2,4-	2.85[a]	3.40[a]	3.19[a]	2.90[a]	4.24[a]	3.08[a]	2.86[a]	2.29[a]	3.29[a]	4.60[a]
	SD	0.98	0.24	1.10	0.54	1.70	0.31	0.83	0.18	0.26	1.08
	3,4-	0.88[a]	0.78[a]	0.67[a]	0.69[a]	0.80[a]	0.70[a]	0.67[a]	0.58[a]	0.55[a]	0.92[a]
	SD	0.35	0.21	0.08	0.19	0.07	0.26	0.25	0.29	0.04	0.07
	2,3,4-	9.17[a]	9.11[a]	6.13[a]	11.78[a]	15.40[a]	12.55[a]	4.77[a]	5.87[a]	5.38[a]	7.38[a]
	SD	9.82	6.12	5.84	11.10	9.57	9.80	1.52	6.98	2.20	2.51
	ΣXyl*p*	**44.23**	**42.44**	**44.05**	**44.90**	**48.94**	**47.21**	**44.57**	**42.23**	**44.50**	**42.27**
Glc*p*A	t-	1.90[a]	2.04[a]	3.56[a]	2.33[a]	3.26[a]	2.52[a]	2.47[a]	1.89[a]	2.35[a]	3.36[a]
	SD	0.14	1.15	1.24	0.73	1.72	0.31	1.08	0.13	0.26	1.05
Ara*f*	t-	0.17[a]	0.87[a]	0.66[a]	0.41[a]	0.71[a]	0.63[a]	0.77[a]	0.42[a]	0.63[a]	0.96[a]
	SD	0.07	0.40	0.31	0.45	0.24	0.20	0.28	0.29	0.12	0.43
	5-	0.81[a]	3.18[a]	1.86[a]	1.64[a]	2.61[a]	1.76[a]	1.57[a]	1.30[a]	1.71[a]	2.97[a]
	SD	0.04	1.08	1.13	1.54	1.10	0.70	0.44	0.65	0.52	1.49
	ΣAra*f*	**0.98**	**4.06**	**2.52**	**2.05**	**3.31**	**2.39**	**2.34**	**1.73**	**2.33**	**3.93**
Man*p*	4-	1.02[a]	1.71[a]	1.14[a]	1.09[a]	1.44[a]	0.97[a]	1.39[a]	1.14[a]	1.42[a]	1.93[a]
	SD	0.11	0.30	0.42	0.41	0.22	0.36	0.30	0.72	0.29	0.82
Rha*p*	3-	0.31[a]	0.71[ab]	0.45[ab]	0.42[ab]	0.85[b]	0.58[ab]	0.31[a]	0.30[a]	0.26[a]	0.79[b]
	SD	0.09	0.11	0.07	0.14	0.19	0.19	0.16	0.18	0.11	0.30
	2,4-	0.24[a]	0.78[ab]	0.36[a]	0.60[a]	0.70[a]	0.74[a]	0.34[a]	0.33[a]	0.47[a]	1.72[b]
	SD	0.08	0.20	0.11	0.14	0.24	0.32	0.23	0.02	0.07	0.88
	ΣRha*p*	**0.55**	**1.49**	**0.82**	**1.02**	**1.54**	**1.32**	**0.65**	**0.63**	**0.73**	**2.51**

Gal*p*	t-SD	0.26[a] 0.12	0.97[a] 0.35	0.50[a] 0.14	0.52[a] 0.29	0.70[a] 0.17	0.62[a] 0.23	0.55[a] 0.14	0.36[a] 0.05	0.51[a] 0.25	1.00[a] 0.51
	3-SD	0.19[a] 0.09	0.45[b] 0.04	0.28[ab] 0.08	0.30[ab] 0.08	0.48[b] 0.11	0.37[ab] 0.13	0.20[a] 0.05	0.19[a] 0.09	0.33[ab] 0.06	0.53[b] 0.05
	2-SD	0.20[a] 0.07	0.52[a] 0.15	0.17[a] 0.11	0.37[a] 0.05	0.19[a] 0.12	0.29[a] 0.13	0.16[a] 0.06	0.19[a] 0.07	0.29[a] 0.13	0.53[a] 0.29
	4-SD	0.21[a] 0.07	0.55[b] 0.13	0.24[ab] 0.13	0.28[ab] 0.10	0.36[ab] 0.08	0.31[ab] 0.11	0.19[a] 0.07	0.17[a] 0.01	0.37[ab] 0.12	0.45[ab] 0.21
	ΣGal*p*	**0.87**	**2.49**	**1.20**	**1.47**	**1.73**	**1.60**	**1.10**	**0.91**	**1.50**	**2.51**
Gal*p*A	t-SD	0.07[ab] 0.02	0.24[b] 0.11	0.07[ab] 0.03	0.13[ab] 0.07	0.13[ab] 0.07	0.08[ab] 0.07	0.04[a] 0.06	0.06[a] 0.02	0.10[ab] 0.02	0.19[ab] 0.06
	2-SD	0.35[a] 0.22	0.43[a] 0.03	0.21[a] 0.09	0.45[a] 0.22	0.56[a] 0.33	0.28[a] 0.13	0.18[a] 0.06	0.28[a] 0.21	0.20[a] 0.10	0.39[a] 0.20
	4-SD	0.41[ab] 0.26	1.76[b] 0.66	0.49[ab] 0.37	0.84[ab] 0.36	1.07[ab] 0.43	0.74[ab] 0.40	0.30[a] 0.15	0.44[ab] 0.19	0.55[ab] 0.41	1.43[ab] 0.93
	ΣGal*p*A	**0.83**	**2.43**	**0.77**	**1.42**	**1.76**	**1.10**	**0.51**	**0.77**	**0.84**	**2.01**

Statistical analysis was done using one-way ANOVA followed by Tukey's multiple comparison test. Statistical significance levels are indicated by letters, with identical letters in the same column denoting no significant difference at the 5% probability level according to the Tukey test. Results are presented as the mean and standard deviation (n = 3). Abbreviations: **Glc*p***: Glucopyranosyl; **Xyl*p***: Xylopyranosyl; **Ara*f***: Arabinofuranosyl; **Rha*p***: Rhamnopyranosyl; **Gal*p***: Galactopyranosyl: **Glc*p*A**: Glucopyranosyl uronic acid; **Gal*p*A**: Galactopyranosylsyl uronic acid; **Man*p***: Mannopyranosyl.

Table 3: Estimation of the amount of xylan and cellulose in the water-insoluble residue (WIR) samples.

Hempseed cultivars	**Xylan (%)**	**Cellulose (%)**
NWG 2730	43.77 ± 4.76[a]	46.80 ± 5.04[a]
Enecterol	40.69 ± 4.99[a]	38.36 ± 1.11[a]
Yuma	42.69 ± 0.49[a]	43.04 ± 1.45[a]
Lara	44.10 ± 4.87[a]	42.16 ± 8.66[a]
Fedora 17	47.37 ± 4.44[a]	35.35 ± 4.68[a]
Henola	45.97 ± 3.52[a]	39.56 ± 5.71[a]
Orion 33	42.86 ± 1.14[a]	43.44 ± 3.08[a]

Futura 75	41.24 ± 6.28[a]	48.27 ± 5.90[a]
Futura 83	43.20 ± 1.64[a]	46.66 ± 4.99[a]
USO 31	40.08 ± 6.15[a]	35.13 ± 4.44[a]

Statistical analysis was done using one-way ANOVA followed by Tukey's multiple comparison test. Statistical significance levels are indicated by letters, with identical letters in the same column denoting no significant difference at the 5% probability level according to the Tukey test. Results are presented as the mean ± standard deviation (n = 3).

Table 4. Major glycosyl linkages (% peak area) of polysaccharides from the water-soluble polysaccharides (WSP) fraction deduced from identified partially methylated alditol acetates (PMAAs). Results are presented as the mean and standard deviation (SD) (n=3).

Glycosyl linkages		**Hempseed Cultivars- Water-soluble Polysaccharides (Area %)**									
		NWG 2730	**Enecterol**	**Yuma**	**Lara**	**Fedora 17**	**Henola**	**Orion 33**	**Futura 75**	**Futura 83**	**USO 31**
Gal*p*	t-	2.86[a]	2.38[a]	2.93[a]	3.12[a]	2.65[a]	2.40[a]	2.81[a]	2.56[a]	1.86[a]	3.10[a]
	SD	0.10	1.27	0.24	0.02	0.16	0.08	0.14	0.05	1.57	0.16
	3-	5.04[a]	6.37[a]	6.46[a]	5.96[a]	6.16[a]	4.81[a]	6.37[a]	5.71[a]	6.66[a]	4.98[a]
	SD	2.63	0.60	0.59	0.39	0.49	0.82	0.29	0.13	0.17	0.21
	2-	0.66[a]	0.51[a]	0.32[a]	0.48[a]	0.67[a]	0.61[a]	0.60[a]	0.78[a]	0.47[a]	1.34[a]
	SD	0.05	0.12	0.14	0.22	0.05	0.04	0.03	0.55	0.05	1.26
	4-	0.93[a]	0.82[a]	1.17[a]	1.59[a]	1.30[a]	1.33[a]	1.10[a]	1.21[a]	1.27[a]	1.48[a]
	SD	0.30	0.61	0.09	0.41	0.16	0.03	0.17	0.24	0.11	0.05
	6-	2.28[ab]	1.89[a]	2.31[ab]	2.26[ab]	2.66[b]	1.65[a]	1.97[ab]	1.98[ab]	2.33[ab]	2.05[ab]
	SD	0.03	0.18	0.36	0.26	0.32	0.21	0.16	0.26	0.32	0.25
	3,4-	0.36[a]	0.49[a]	0.20[a]	0.67[a]	0.45[a]	0.70[a]	0.31[a]	0.50[a]	0.53[a]	0.39[a]
	SD	0.05	0.11	0.06	0.33	0.10	0.12	0.19	0.44	0.12	0.11
	3,6-	16.57[cd]	13.14[abc]	14.93[bcd]	12.51[ab]	16.92[d]	11.80[ab]	12.50[ab]	12.38[ab]	14.52[bcd]	10.37[a]
	SD	1.64	0.66	0.90	1.21	1.90	1.53	1.04	0.57	1.68	0.72
	ΣGal*p*	**28.71**	**25.60**	**28.32**	**26.59**	**30.80**	**23.29**	**25.65**	**25.12**	**27.63**	**23.71**

Ara*f*	t-	7.46^{a}	11.15^{a}	9.25^{ab}	10.94^{a}	5.37^{b}	9.68^{a}	9.53^{a}	9.81^{a}	10.57^{a}	8.03^{ab}
	SD	2.19	0.78	2.02	1.86	1.68	0.33	0.24	1.28	1.10	0.91
	3-	0.30^{a}	0.42^{a}	0.33^{a}	0.44^{a}	0.38^{a}	0.36^{a}	0.32^{a}	0.36^{a}	0.46^{a}	0.37^{a}
	SD	0.00	0.08	0.06	0.08	0.04	0.07	0.08	0.07	0.07	0.07
	5-	11.86^{bc}	12.76^{c}	12.84^{c}	10.05^{ab}	9.77^{ab}	10.71^{bc}	9.84^{ab}	11.82^{bc}	11.64^{bc}	8.18^{a}
	SD	0.56	0.91	0.88	1.45	0.11	0.98	0.93	0.21	0.77	0.89
	2,5-	2.23^{a}	2.00^{a}	2.32^{a}	1.61^{a}	2.20^{a}	1.50^{a}	1.69^{a}	2.21^{a}	2.04^{a}	1.68^{a}
	SD	1.01	0.47	0.33	0.74	0.38	0.36	0.39	0.15	0.01	0.23
	Σ Ara*f*	**21.85**	**26.33**	**24.73**	**23.03**	**17.72**	**22.25**	**21.38**	**24.20**	**24.71**	**18.27**
Man*p*	t-	4.69^{a}	5.16^{a}	5.22^{a}	5.16^{a}	5.07^{a}	7.35^{a}	7.91^{a}	5.41^{a}	7.22^{a}	6.51^{a}
	SD	1.93	1.52	1.67	1.50	1.85	0.92	2.50	1.40	1.18	1.85
	2-	2.99^{a}	3.62^{a}	3.82^{a}	4.20^{a}	3.99^{a}	5.53^{a}	4.98^{a}	3.95^{a}	4.30^{a}	5.50^{a}
	SD	0.52	1.02	0.63	0.71	1.01	0.13	1.28	1.26	0.83	1.13
	4-	7.42^{b}	4.41^{a}	4.97^{ab}	5.23^{ab}	6.31^{ab}	4.47^{a}	5.13^{ab}	4.57^{a}	4.34^{a}	5.17^{ab}
	SD	2.06	0.23	0.79	0.73	1.22	0.24	0.19	0.62	0.41	0.76
	6-	0.62^{a}	0.54^{a}	0.47^{a}	0.70^{a}	1.09^{a}	0.95^{a}	1.06^{a}	0.39^{a}	0.50^{a}	1.20^{a}
	SD	0.21	0.21	0.30	0.15	0.09	0.15	0.16	0.36	0.04	1.09
	2,3-	1.91^{abc}	1.47^{a}	1.55^{a}	1.85^{abc}	2.16^{bc}	2.02^{ab}	1.60^{a}	1.70^{ab}	1.65^{ab}	2.28^{c}
	SD	0.34	0.01	0.35	0.04	0.11	0.09	0.16	0.24	0.11	0.09
	2,6-	1.41^{a}	0.96^{a}	1.02^{a}	1.05^{a}	1.58^{a}	1.44^{a}	1.77^{a}	1.16^{a}	1.48^{a}	1.77^{a}
	SD	0.65	0.43	0.49	0.49	0.52	0.32	0.68	0.50	0.21	0.67
	Σ Man*p*	**19.05**	**16.15**	**17.05**	**18.19**	**20.21**	**21.75**	**22.45**	**17.18**	**19.48**	**22.42**

Glc*p*	t-	1.65^{ab}	2.40^{abc}	1.47^{a}	2.97^{bc}	2.19^{abc}	3.35^{cd}	3.20^{cd}	2.57^{abc}	2.33^{abc}	4.44^{d}
	SD	0.09	0.75	0.97	0.24	0.38	0.20	0.42	0.33	0.36	0.24
	3-	0.90^{ab}	0.70^{a}	0.79^{a}	1.24^{ab}	0.77^{a}	0.95^{ab}	0.85^{a}	0.93^{ab}	0.70^{a}	1.83^{b}
	SD	0.01	0.17	0.33	0.29	0.08	0.11	0.33	0.20	0.08	0.85
	2-	0.16^{a}	0.17^{a}	0.18^{a}	0.29^{ab}	0.27^{ab}	0.28^{ab}	0.23^{ab}	0.25^{ab}	0.15^{a}	0.37^{b}
	SD	0.05	0.05	0.03	0.04	0.06	0.09	0.02	0.04	0.03	0.05
	4-	8.51^{a}	8.73^{a}	7.60^{a}	9.72^{a}	8.96^{a}	10.03^{a}	9.05^{a}	11.83^{a}	6.55^{a}	9.58^{a}
	SD	3.63	2.66	2.03	3.73	3.71	3.65	2.19	2.57	2.11	3.43
	3,4-	0.12^{ab}	0.57^{ab}	0.09^{ab}	0.61^{ab}	0.30^{ab}	0.47^{ab}	0.02^{a}	0.79^{b}	0.15^{ab}	0.46^{ab}
	SD	0.16	0.52	0.15	0.16	0.11	0.22	0.02	0.53	0.09	0.01
	2,4-	0.46^{a}	1.02^{a}	0.36^{a}	0.71^{a}	0.70^{a}	0.62^{a}	0.44^{a}	0.44^{a}	0.46^{a}	0.63^{a}
	SD	0.05	0.66	0.06	0.24	0.06	0.11	0.12	0.01	0.08	0.18
	3,6-	0.77^{a}	0.49^{a}	0.54^{a}	0.60^{a}	0.99^{a}	0.93^{a}	0.79^{a}	0.67^{a}	0.74^{a}	1.01^{a}
	SD	0.21	0.15	0.14	0.06	0.24	0.25	0.22	0.29	0.17	0.29
	4,6-	1.52^{a}	0.79^{a}	1.01^{a}	0.82^{a}	1.56^{a}	1.12^{a}	1.04^{a}	1.04^{a}	1.13^{a}	1.00^{a}
	SD	0.33	0.20	0.36	0.11	0.25	0.43	0.17	0.02	0.34	0.21
	ΣGlc*p*	**14.08**	**14.86**	**12.03**	**16.95**	**15.72**	**17.76**	**15.62**	**18.52**	**12.21**	**19.32**
Xyl*p*	t-	2.74^{ab}	2.25^{abc}	2.50^{abc}	1.70^{c}	1.87^{bc}	1.91^{abc}	2.13^{abc}	2.49^{abc}	2.84^{a}	2.23^{abc}
	SD	0.46	0.33	0.40	0.13	0.39	0.05	0.19	0.20	0.46	0.36
	4-	2.56^{a}	3.17^{a}	4.41^{a}	2.82^{a}	2.30^{a}	2.31^{a}	2.17^{a}	3.20^{a}	2.27^{a}	3.01^{a}
	SD	0.93	1.51	2.21	0.32	0.58	0.31	0.25	1.34	0.06	1.11
	2-	0.38^{ab}	0.64^{b}	0.43^{ab}	0.48^{ab}	0.39^{ab}	0.45^{ab}	0.54^{ab}	0.46^{ab}	0.22^{a}	0.44^{ab}
	SD	0.10	0.24	0.16	0.08	0.05	0.05	0.14	0.13	0.21	0.01
	ΣXyl*p*	**5.69**	**6.06**	**7.34**	**5.00**	**4.56**	**4.68**	**4.84**	**6.15**	**5.32**	**5.67**
Glc*p*A	t-	0.99^{a}	0.91^{a}	1.65^{a}	1.12^{a}	1.23^{a}	0.77^{a}	0.93^{a}	0.79^{a}	1.08^{a}	0.95^{a}
	SD	0.10	0.09	0.86	0.20	0.12	0.42	0.08	0.07	0.14	0.26
	4-	2.20^{b}	1.68^{a}	1.68^{a}	1.75^{a}	2.30^{c}	1.77^{ab}	1.94^{abc}	1.64^{a}	1.53^{a}	1.65^{a}
	SD	0.20	0.15	0.12	0.07	0.11	0.04	0.15	0.29	0.06	0.16
	3,4-	1.09^{c}	0.41^{a}	0.66^{abc}	0.32^{a}	0.85^{b}	0.59^{ab}	0.76^{abc}	0.32^{a}	0.68^{abc}	0.51^{ab}
	SD	0.18	0.16	0.06	0.14	0.12	0.03	0.23	0.27	0.09	0.01
	ΣGlc*p*A	**4.29**	**2.99**	**3.99**	**3.20**	**4.37**	**3.13**	**3.63**	**2.74**	**3.29**	**3.10**

Gal*p*A	t-	0.28[a]	0.78[a]	0.25[a]	0.44[a]	0.41[a]	0.38[a]	0.34[a]	0.26[a]	1.25[a]	0.56[a]
	SD	0.07	0.68	0.09	0.03	0.07	0.27	0.12	0.04	1.70	0.27
	4-	2.40[a]	3.25[a]	2.63[a]	2.82[a]	2.61[a]	2.44[a]	2.39[a]	2.27[a]	2.47[a]	2.56[a]
	SD	0.89	0.76	0.76	0.20	0.25	0.11	0.20	0.15	0.21	0.43
	3,4-	0.40[a]	0.44[a]	0.65[a]	0.62[a]	0.47[a]	0.57[a]	0.67[a]	0.36[a]	0.50[a]	0.81[a]
	SD	0.09	0.16	0.20	0.20	0.05	0.16	0.09	0.35	0.13	0.22
ΣGal*p*A		**3.08**	**4.47**	**3.53**	**3.88**	**3.49**	**3.39**	**3.40**	**2.90**	**4.22**	**3.93**
Rha*p*	t-	1.22[a]	1.60[a]	1.25[a]	1.16[a]	1.20[a]	1.35[a]	1.31[a]	1.31[a]	1.20[a]	1.24[a]
	SD	0.19	0.30	0.23	0.37	0.28	0.23	0.33	0.16	0.29	0.02
	2-	0.62[a]	0.74[a]	0.59[a]	0.67[a]	0.61[a]	0.71[a]	0.58[a]	0.56[a]	0.69[a]	0.69[a]
	SD	0.17	0.30	0.17	0.11	0.13	0.10	0.11	0.03	0.16	0.14
	2,4-	0.76[a]	0.59[a]	0.63[a]	0.72[a]	0.61[a]	0.80[a]	0.55[a]	0.67[a]	0.67[a]	0.79[a]
	SD	0.19	0.05	0.15	0.23	0.13	0.03	0.05	0.08	0.19	0.24
ΣRha*p*		**2.59**	**2.93**	**2.47**	**2.55**	**2.42**	**2.87**	**2.44**	**2.54**	**2.55**	**2.72**
Fuc*p*	t-	0.41[a]	0.39[a]	0.35[a]	0.37[a]	0.37[a]	0.57[a]	0.37[a]	0.44[a]	0.35[a]	0.46[a]
	SD	0.09	0.03	0.07	0.04	0.07	0.10	0.05	0.06	0.13	0.09
Api*f*	3'-	0.26[ab]	0.22[ab]	0.19[a]	0.24[ab]	0.32[ab]	0.31[ab]	0.23[ab]	0.22[ab]	0.24[ab]	0.41[b]
	SD	0.08	0.07	0.03	0.09	0.05	0.06	0.01	0.07	0.05	0.12

Statistical analysis was done using one-way ANOVA followed by Tukey's multiple comparison test. Statistical significance levels are indicated by letters, with identical letters in the same row denoting no significant difference at the 5% probability level according to the Tukey test. Results are presented as the mean and standard deviation (n = 3). Abbreviations: **Gal*p***: Galactopyranosyl; **Ara*f***: Arabinofuranosyl; **Man*p***: Mannopyranosyl; **Glc*p***: Glucopyranosyl; **Xyl*p***: Xylopyranosyl; **Glc*p*A**: Glucopyranosyl uronic acid; **Gal*p*A**: Galactopyranosyl uronic acid; **Rha*p***: Rhamnopyranosyl; **Fuc*p***: Fucopyranosyl; **Api*f***: Apiofuranosyl.

NMR Analysis

Since the bulk of whole hempseed's polysaccharides are water-insoluble and therefore ill-suited for traditional solution-state NMR analysis, we ball-milled and then directly swelled the finely-ground WIR materials into a gel in DMSO-d_6 (Kim et al., 2008). The 2D-HSQC-NMR spectra with good resolution were acquired from these gels, revealing the polysaccharides in their native cell wall context. Because these are cell wall samples, lignin and protein signals are also clearly present in the spectra, but detailed structural analysis of these polymers is outside the scope of this work. The intent of NMR analysis was to confirm

the overall cell wall carbohydrate makeup of whole hempseeds projected by the methylation and monosaccharide compositional analyses and to provide complementary structural details to the wet chemistry results. Individual peaks within a “gel-state” spectrum should not be compared in a strictly quantitative fashion for two reasons: first, signals from terminal ends and pendant units on the polysaccharides are magnified due to the slower relaxation rate of these units compared to the rapid relaxation of the bulk polymers in the gel (Mansfield et al., 2012). Incidentally, the rapid relaxation of the bulk polymers in the gel renders these samples unsuitable for some 2D-NMR experiments that require longer delay periods to allow for evolution of long-range coupling, such as HMBC, since if relaxation happens too quickly, magnetization decays before it can be transferred. Second, crystalline cellulose is underrepresented in the spectra since it does not swell substantially in the DMSO solvent (Kim et al., 2008; Mansfield et al., 2012). Nevertheless, the spectra are reproducible, meaning that samples prepared, measured, and processed in the same way may be compared with each other.

As anticipated by the monosaccharide composition and methylation results, the anomeric regions of the WIR spectra (see Figure 4A and Supplementary Figure S4) contained an intense, broad signal from the internal 1,4-β-Xyl*p* residues of β-(1→4)-linked xylans (~101.6/4.28 ppm), signals from the α- and β-Xyl*p* reducing ends of xylans (~92.0/4.83 ppm and 97.2/4.23 ppm, respectively), and signals corresponding to the 1,4-β-Glc*p* residues of cellulose (~103.0/4.16 ppm for non-reducing ends, ~102.8/4.30 ppm for internal residues), which were assigned by comparison with literature data from cellulose and xylans in DMSO-d_6 (Kim & Ralph, 2014). Additionally, acetylation of xylans, a structural element which is not detected by methylation or monosaccharide composition analyses, was readily observed in all WIR spectra **(Figure 4A)**. The methyl group from acetyl was present at ~20.7/2.01 ppm, consistent with acetylated polysaccharides, and strong signals from mono- and di-acetylated β-Xyl*p* residues were evident both in the anomeric (~99.4/4.49 ppm, 2-*O*-Ac-β-Xyl*p*; 101.4/4.40 ppm, 3-*O*-Ac-β-Xyl*p*; 98.7/4.70 ppm, 2,3-di-*O*-Ac-β-Xyl*p*) and *O*-acetylated carbohydrate regions (~73.3/4.48 ppm, C2/H2 from 2-*O*-Ac-β-Xyl*p*; ~74.7/4.78 ppm, C3/H3 from 3-*O*-Ac-β-Xyl*p*; 71.0/4.60 ppm and 72.5/4.94 ppm, C2/H2 and C3/H3, respectively, of 2,3-di-*O*-Ac-β-Xyl*p*) of the WIR from all the hempseed varieties and corresponded closely to reported literature data (Kim & Ralph, 2014; Rencoret et al., 2018; Teleman et al., 2000). NOESY analysis of the gel-state sample revealed a crosspeak between the methyl protons of the acetyl group (2.00 ppm) and the signal assigned as H2 of 2-*O*-Ac-β-Xyl*p* (4.48 ppm), indicating spatial proximity between these constituents **(Supplementary Figure S6)**. The distinctive anomeric peak for non-reducing terminal 4-*O*-methyl-α-Glc*p*A was present at ~97.1/5.15 ppm, as well as the anomeric peak from β-Xyl*p* branched with 4-*O*-methyl-α-Glc*p*A (~101.7/4.75 ppm) and the methoxyl group from 4-*O*-methyl-α-Glc*p*A (~59.6/3.36 ppm) (Kim & Ralph, 2014; Teleman et al., 2000). Two anomeric peaks corresponding to 1,5-

α-Ara*f* were clearly visible (~107.9/4.75 and 107.2/4.89 ppm), underlining the presence of pectic arabinans in the samples, as well as small signals corresponding to β-Gal*p* (~105.0/4.29 ppm) and β-Man*p* (~100.8/4.61 ppm). The origin of two small peaks in the anomeric region at ~98.9/5.06 ppm and ~102.9/4.49 ppm could not be assigned from literature values for carbohydrates in DMSO-d_6. It is possible that the small unidentified peak in the alpha-anomer region arose from 4- and 4,6-linked α-Glc*p*, e.g. the small amounts of residual starch in the sample, but the ^{13}C shift is upfield from reported literature values for glycosidic linkages in starch: 100.4/5.21 ppm and 99.8-100.1/5.07-5.11 ppm in DMSO-d_6 and DMSO-d_6/pyridine-d_5 (4:1, v/v), respectively (Falk & Stanek, 1997; Unda et al., 2017).

To confirm the acetylation pattern on the water-insoluble xylans, acetylated xylans were extracted from the WIR with DMSO following a mild delignification with peracetic acid and subsequently digested with pure endo-1,4-β-xylanase to generate xylooligosaccharides (XOS). Comprehensive 2D-NMR analyses including HSQC, HMBC, COSY, and HSQC-TOCSY (**Figure 5; Supplementary Figures S7 and S8**) performed on both the extracted xylan material and the resulting XOS verified the acetylation positions and anomeric assignments of the acetylated xyloses. In particular, HMBC analysis showed cross-peaks corresponding to the methyl protons of acetyl and C2 of 2-*O*-Ac-β-Xyl*p*, C3 of 3-*O*-Ac-β-Xyl*p* and C2 and C3 of 2,3-di-*O*-Ac-β-Xyl*p* **(Figure 5B)**. Additionally, we observed clear HMBC crosspeaks between the four protons at the acetylated positions of xylose units (e.g., H2 of 2-*O*-Ac-β-Xyl*p*, H3 of 3-*O*-Ac-β-Xyl*p*, and H2 and H3 from 2,3-di-*O*-Ac-β-Xyl*p*) and an acetyl carbonyl group (169.4 ppm), data not shown. HSQC-TOCSY of these isolated samples allowed us to assign carbon shifts to the ring system of each xylose type and confirmed the anomeric assignments for the xyloses in the gel-state samples **(Supplementary Figures S7 and S8)**. The endoxylanase-generated oligosaccharides also contained 4-*O*-methyl-α-Glc*p*A units, and the additional 2D-NMR analyses corroborated the assignments of its methoxyl and anomeric signals and permitted some additional assignments, including the methoxylated C4/H4 (81.2/3.07 ppm; Figure 5A). Some non-xylose signals were seen in the enzymatic hydrolysates, which likely arose from minor coextraction of glucose-containing polysaccharides in the PAA/DMSO-based xylan extraction procedure that were then re-solubilized into the enzymatic hydrolysate.

To facilitate comparison with the WIR spectra, WSP were also dissolved and analyzed in DMSO-d_6. In contrast to the WIR spectra, no acetylation of carbohydrates was observed in the spectra from the WSP samples **(Figure 4B and Supplementary Figure S5)**. Some glycosyl units observed in the monosaccharide composition and/or linkage composition analysis, such as fucose, apiose, glucuronic acid, and galacturonic acid were not identified in the spectra due to either low concentrations and signal intensity or overlap with other signals. Peaks corresponding to 1,4-β-Glc*p* (~103.3/4.14 ppm for non-reducing ends and ~102.6/4.331 ppm for internal residues), β-Gal*p* (~104.1/4.14 ppm and 105.0/4.29 ppm), and β-Man*p*,

630 which were identified by comparison to literature data (Brennan et al., 2012; Golovchenko et al., 2024;
631 Kim & Ralph, 2014; Lucyszyn et al., 2011; Shakhmatov et al., 2017), were visible in the beta-anomer
632 region, but in strong contrast to the WIR spectra, 1,4-β-Xyl*p* did not appear above the background noise.
633 Signals from the α- and β-Gal*p* reducing ends of galactans (~91.3/5.17 and ~96.7/4.25 ppm, respectively)
634 were also seen. Similarly to the WIR samples, 1,5-α-Ara*f* was clearly present, and an additional downfield
635 signal corresponding to terminal α-Ara*f* (~108.8/5.05 ppm) appeared. The alpha-anomer region also
636 contained terminal α-Rha*p* (~99.8/4.56 ppm). Several signals in the anomeric region could not be identified.
637 More in-depth NMR structural confirmation of all the branching patterns contained in the WSP would
638 require scaled-up purification, concentration of the separate polysaccharides to increase signal intensity and
639 resolution, and additional 2D experiments (e.g., COSY, HMBC, HSQC-TOCSY). However, since the
640 primary goal of this study was to provide a broad characterization of hempseed cell walls across 10 varieties
641 to inform predictions about their functionality and potential applications in food and biomaterials, we did
642 not conduct exhaustive NMR characterization of the minor polysaccharides in the already-minor WSP
643 fractions at this time.

644

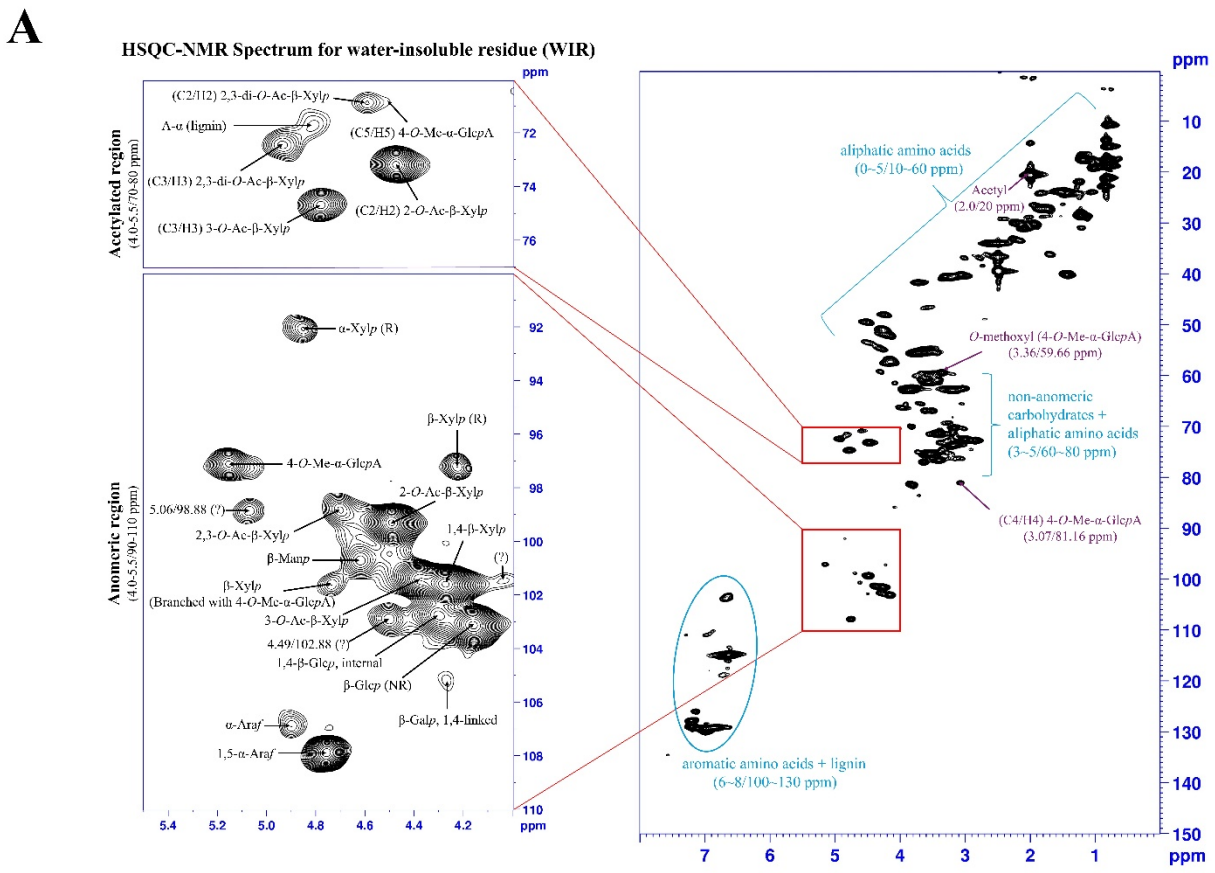

645

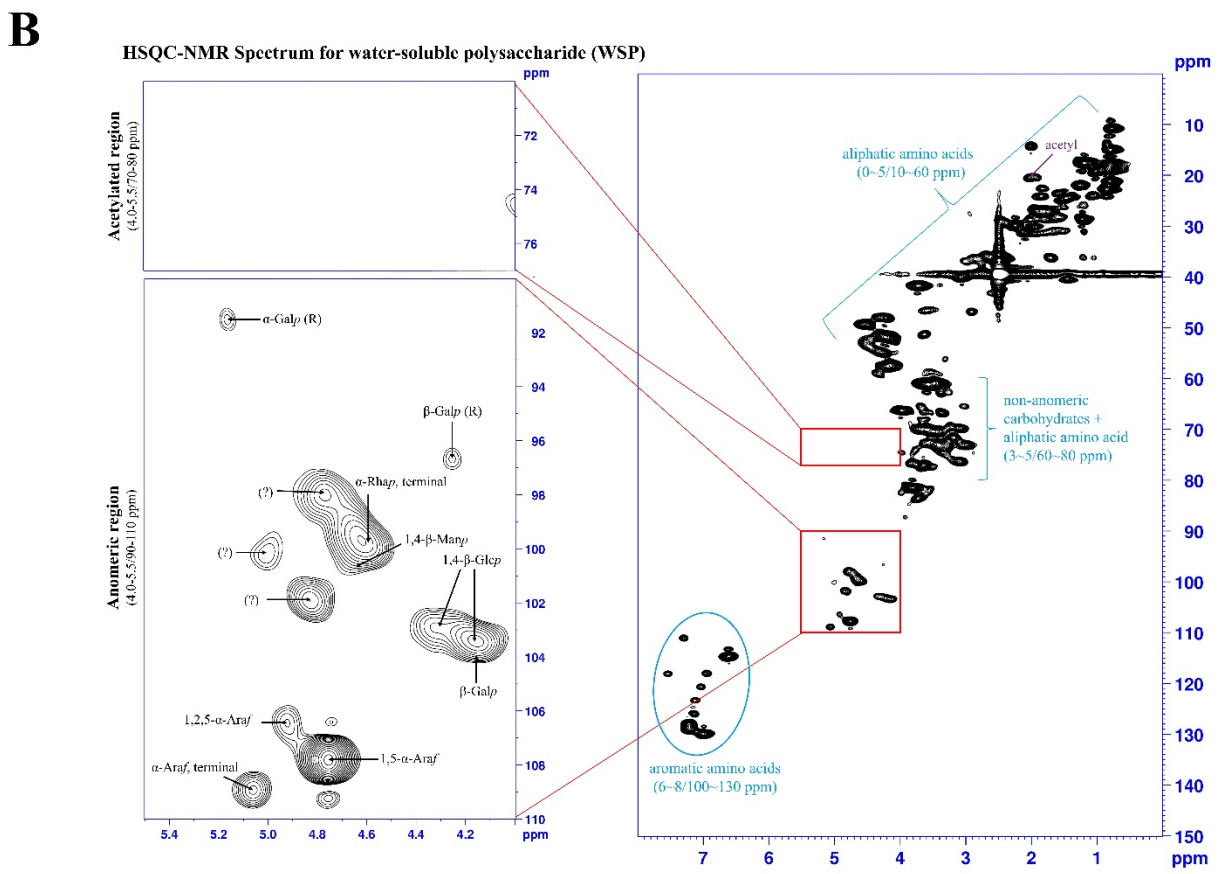

Figure 4. Representative 2D ^{13}C-^{1}H (HSQC)-NMR spectra of gels prepared from (A) water-insoluble residues (WIR) and (B) water-soluble polysaccharides (WSP) isolated from the hempseed variety "USO 31" in DMSO-d_6, highlighting the anomeric and *O*-acetylated carbohydrate regions. Spectra were calibrated against DMSO (δH = 2.49 ppm, δC = 39.50 ppm). Abbreviations used: α-Ara*f*, α-arabinofuranoside; β-Glc*p*, β-glucopyranoside; β-Gal*p*, β-galactopyranoside; β-Man*p*, β-mannopyranoside; 4-*O*-Me-α-Glc*p*A, 4-*O*-methyl-α-glucuronic acid; α-Rha*p*, α-rhamnopyranoside; α-Xyl*p*, α-xylopyranoside; β-Xyl*p*, β-xylopyranoside; 2-*O*-Ac-β-Xyl*p*, 2-*O*-monoacetylated-β-xylopyranoside; 3-*O*-Ac-β-Xyl*p*, 3-*O*-monoacetylated-β-xylopyranoside; (R), reducing end; (NR), non-reducing end.

A

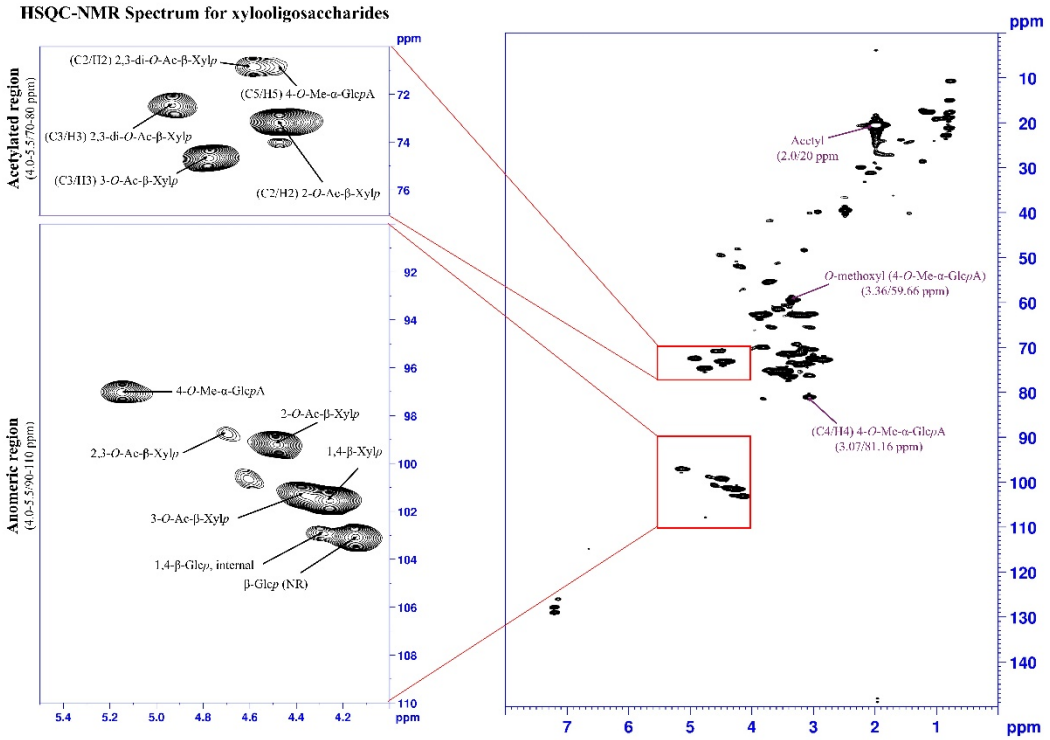
HSQC-NMR Spectrum for xylooligosaccharides
Acetylated region
(4.0-5.5/70-80 ppm)
(C2/H2) 2,3-di-O-Ac-β-Xylp
(C5/H5) 4-O-Me-α-GlcpA
(C3/H3) 2,3-di-O-Ac-β-Xylp
(C3/H3) 3-O-Ac-β-Xylp
(C2/H2) 2-O-Ac-β-Xylp
Anomeric region
(4.0-5.5/90-110 ppm)
4-O-Me-α-GlcpA
2-O-Ac-β-Xylp
2,3-O-Ac-β-Xylp
1,4-β-Xylp
3-O-Ac-β-Xylp
1,4-β-Glcp, internal
β-Glcp (NR)
Acetyl
(2.0/20 ppm
O-methoxyl (4-O-Me-α-GlcpA)
(3.36/59.66 ppm)
(C4/H4) 4-O-Me-α-GlcpA
(3.07/81.16 ppm)
ppm

656

B

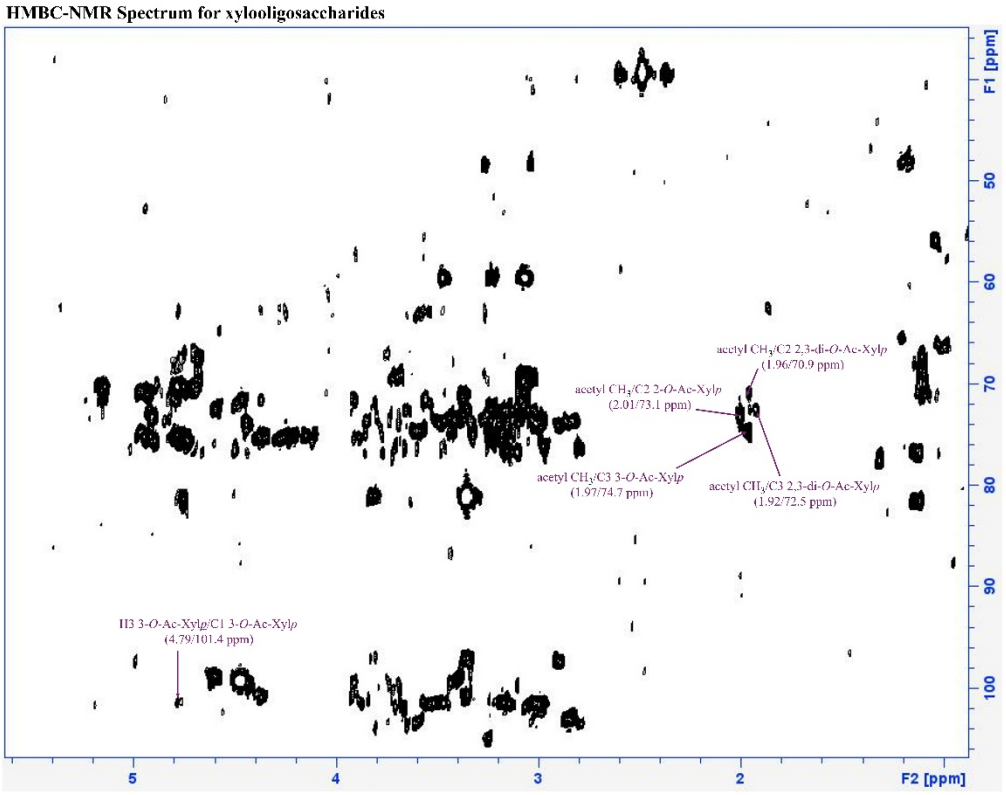
HMBC-NMR Spectrum for xylooligosaccharides
acetyl CH3/C2 2,3-di-O-Ac-Xylp
(1.96/70.9 ppm)
acetyl CH3/C2 2-O-Ac-Xylp
(2.01/73.1 ppm)
acetyl CH3/C3 3-O-Ac-Xylp
(1.97/74.7 ppm)
acetyl CH3/C3 2,3-di-O-Ac-Xylp
(1.92/72.5 ppm)
H3 3-O-Ac-Xylp/C1 3-O-Ac-Xylp
(4.79/101.4 ppm)
F1 [ppm]
F2 [ppm]

657

Figure 5. HSQC-NMR and HMBC-NMR spectra of xylooligosaccharides (XOS) dissolved in DMSO-*d*$_6$. The XOS were generated via enzymatic digestion of isolated xylans from the water-insoluble residue (WIR) using endo-1,4-β-xylanase. (A) HSQC spectrum highlights the anomeric and *O*-acetylated carbohydrate regions. (B) HMBC spectrum illustrating acetylation of xylans at the *O*-2 and *O*-3 positions. Chemical shifts were calibrated using residual DMSO (δH = 2.49 ppm, δC = 39.50 ppm). Abbreviations: 4-*O*-Me-α-GlcpA, 4-*O*-methyl-α-glucuronic acid; β-Xylp, β-D-xylopyranoside; 2-*O*-Ac-β-Xylp, 2-*O*-acetyl-β-D-xylopyranoside; 3-*O*-Ac-β-Xylp, 3-*O*-acetyl-β-D-xylopyranoside; (NR), non-reducing end.

Functionality of Hempseed Fiber in Food Products

Our cultivar profiling shows that whole hempseeds consistently contain abundant cell wall polysaccharide material, regardless of cultivar type. The rich fiber content of whole hempseed-based ingredients, like ground hempseed flour, makes them appealing to food manufacturers aiming to create products high in dietary fiber for health-conscious consumers since modest inclusion rates of hempseed in a formula can still produce a higher declared dietary fiber content per serving compared to control products made from refined wheat flour. Indeed, numerous research groups have recently published evaluations of fiber-enriched food products fortified with whole hempseed flour or hempseed cake, including pasta (Bonacci et al., 2023; Teterycz et al., 2021), gnocchi (Merlino et al., 2022), bread (Korus et al., 2017; Mikulec et al., 2019; Pojić et al., 2015; Sciacca et al., 2023), cookies (Ertaş & Aslan, 2020), and extruded snacks (Norajit et al., 2011).

Water-soluble fiber polysaccharides increase solution viscosity and can be used as thickeners or gel-forming ingredients in food products. Although water-insoluble fiber does not affect solution viscosity, it still binds and absorbs water (Föste et al., 2020), reducing water's availability to hydrate other food components, such as protein and starch, and creating techno-functional challenges in baked goods (Wang et al., 2023). Higher insoluble fiber content also reduces expansion during extrusion, resulting in harder and more dense extruded products (Kale et al., 2011; Woomer et al., 2023). Because of hempseed's high insoluble fiber content, targeted fiber processing strategies to mitigate negative effects will enable its successful incorporation into food products. Specifically, particle size reduction and modifications that convert at least some of the insoluble fiber polysaccharides to water-soluble polymers have been observed to enhance the functionality of insoluble fibers (Bader Ul Ain et al., 2019; Robin et al., 2012). Various milling and grinding techniques targeted towards particle size reduction of insoluble fiber have been described (Bader Ul Ain et al., 2019; Chau et al., 2007; Chau et al., 2006; Ma & Mu, 2016). Enzymatic treatments (e.g., xylanase, cellulase, lignin oxidase) can shift the ratio of soluble: insoluble fiber (Bader Ul Ain et al., 2019; Föste et al., 2020;

Luo et al., 2018), and microbial pre-fermentation can improve hydration properties and also activate endogenous enzymes via the reduction in pH (Bader Ul Ain et al., 2019). Pre-soaking of fiber prior to mixing it with other ingredients has also been shown to reduce negative effects (Föste et al., 2020).

Additionally, hempseed was identified as a rich source of linear acetylated xylans, containing approximately 40% to 47% of xylan in the WIR fractions **(Table 3)**. This suggests its potential as a source of extracted xylan. Xylans with a comparable structure are found in wood, and following their extraction from the wood matrix under alkaline conditions, they have been shown to have emulsion-stabilizing and probiotic functionality (Abik et al., 2023; Sedlmeyer, 2011).

Conclusion

All the analyzed hempseed cultivars exhibited high cell wall contents, predominantly comprising water-insoluble fiber material. The study revealed strong consistency across all hemp cultivars, which were found to have a comparable non-starch polysaccharide composition in their seeds, with the cell walls being dominated by linear acetylated xylans and cellulose. Acetylation of hempseed xylans occurs at *O*-2 (2-*O*-Ac-Xyl*p*), *O*-3 (3-*O*-Ac-Xyl*p*), and both the *O*-2 and *O*-3 positions (2,3-di-*O*-Ac-Xyl*p*) of xylosyl residues, and xylans were also substituted with 4-*O*-methyl-α-Glc*p*A. A small amount of other polysaccharides were also identified, including heteromannans, pectic polysaccharides (rhamnogalacturonans and xylogalacturonan), arabinogalactans, and xyloglucans, particularly in the less abundant water-soluble cell wall material. Lignin also made up a significant proportion of the cell wall material. **Figure 6** summarizes our comprehensive findings of the hempseed cell wall components based on Sticklen's model (Sticklen, 2008). The structural elucidation of hempseed cell wall polysaccharides provides a foundational framework for potential future applications in nutrition, biofuel, and various industrial contexts.

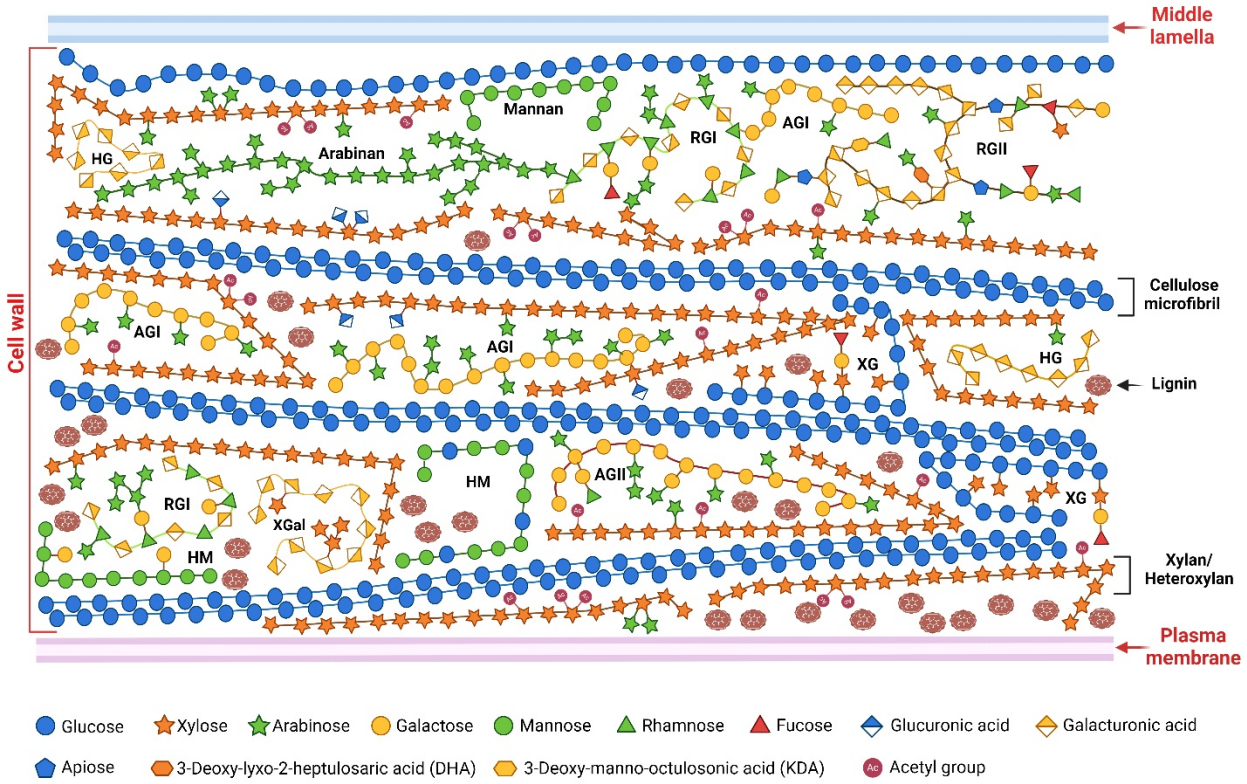

Figure 6. Conceptual illustration of structural features of the hempseed cell wall. Hempseed cell walls comprise cellulose and hemicelluloses such as xylan, mannan, heteromannan (glucomannan or galactoglucomannan), and xyloglucan. Pectins (rhamnogalacturonans, arabinogalactans, and arabinan) are also present. This illustration is based on Sticklen's model of the dicot cell wall (Sticklen, 2008) and was created with BioRender.com. The monosaccharide composition and linkage patterns shown in this figure correspond to the results obtained through compositional, linkage, and NMR analyses in this study. **XG**: Xyloglucan; **HM**: Heteromannan; **AGI**: Arabinogalactan type I; **AGII**: Arabinogalactan type II; **RGI**: Rhamnogalacturonan type I; **RGII**: Rhamnogalacturonan type II; **HG**: Homogalacturonan; **XGal**: Xylogalacturonan.

Acknowledgements

The authors gratefully acknowledge Dr. Robert Pearce from the University of Kentucky for generously providing harvested seeds from the cultivars analyzed in this study and experimental support. We also extend our sincere thanks to Dr. John Ralph from the Wisconsin Energy Institute, University of Wisconsin-Madison, for access to agate ball-milling and NMR facilities, as well as for his valuable insights.

Additionally, we are grateful to Dr. Vivekanandan Subramanian from the PharmNMR Center, College of Pharmacy, University of Kentucky, for analytical support in NMR experiments. We also thank Miranda Agbana for constructive discussions.

Funding

This study was funded by the U.S. Department of Agriculture (USDA), Agricultural Research Service as part of National Program 215; Grass, Forage, and Rangeland Agroecosystems (Project #: 5042-21000-003-00D). USDA is an equal opportunity provider and employer. Additional financial support for this work was provided by the National Institute of Food and Agriculture, U.S. Department of Agriculture, Hatch Program project KY007112 under accession #1021937. Work at the Complex Carbohydrate Research Center was supported by the U.S. Department of Energy, Office of Science, Basic Energy Sciences, Chemical Sciences, Geosciences, and Biosciences Division, under award #DE-SC0015662. NMR analytical work at the PharmNMR Center of the College of Pharmacy, University of Kentucky is supported in part by NIH grants S10 OD28690 and P20 GM130456. NMR analytical work at the Wisconsin Energy Institute was supported in part by the Great Lakes Bioenergy Research Center, U.S. Department of Energy, Office of Science, Biological and Environmental Research Program under Award Number DE-SC0018409.

References

Abik, F., Palasingh, C., Bhattarai, M., Leivers, S., Strom, A., Westereng, B., Mikkonen, K. S., & Nypelo, T. (2023). Potential of wood hemicelluloses and their derivates as food ingredients. *Journal of Agricultural and Food Chemistry*, *71*(6), 2667-2683.

Aboughe-Angone, S., Nguema-Ona, E., Boudjeko, T., & Driouich, A. (2011). Plant cell wall polysaccharides: Immunomodulators of the immune system and source of natural fibers. *Phytochemistry*, *20*, 1-16.

Agbana, M. R., Angeletti, B. S., Buecker, H. C., Tseng, Y.-C., Davis, B. E., & Schendel, R. R. (2024). Characterizing the non-starch polysaccharides of hempseed cell walls. *European Food Research and Technology*, 1-15.

Albersheim, P., Darvill, A., Robert, K., Sederoff, R., & Staehelin, A. (2010). *Plant Cell Walls*. Garland Science, Taylor & Francis Group, LLC. https://doi.org/https://doi.org/10.1201/9780203833476

Alonso-Esteban, J. I., Pinela, J., Ćirić, A., Calhelha, R. C., Soković, M., Ferreira, I. C., Barros, L., Torija-Isasa, E., & de Cortes Sánchez-Mata, M. (2022). Chemical composition and biological activities of whole and dehulled hemp (*Cannabis sativa* L.) seeds. *Food Chemistry*, *374*, 131754.

Alonso-Sande, M., Teijeiro-Osorio, D., Remuñán-López, C., & Alonso, M. (2009). Glucomannan, a promising polysaccharide for biopharmaceutical purposes. *European Journal of Pharmaceutics and Biopharmaceutics*, *72*(2), 453-462.

Andersson, A. A., Lampi, A.-M., Nystrom, L., Piironen, V., Li, L., Ward, J. L., Gebruers, K., Courtin, C. M., Delcour, J. A., & Boros, D. (2008). Phytochemical and dietary fiber components in barley varieties in the HEALTHGRAIN diversity screen. *Journal of Agricultural and Food Chemistry*, *56*(21), 9767-9776.

Bader Ul Ain, H., Saeed, F., Ahmed, A., Asif Khan, M., Niaz, B., & Tufail, T. (2019). Improving the physicochemical properties of partially enhanced soluble dietary fiber through innovative techniques: A coherent review. *Journal of Food Processing and Preservation*, *43*(4), e13917.

Barnes, W. J., & Anderson, C. T. (2017). Acetyl bromide soluble lignin (ABSL) assay for total lignin quantification from plant biomass. *Bio-protocol*, *7*(5), e2149-e2149.

Black, I. M., Ndukwe, I. E., Vlach, J., Backe, J., Urbanowicz, B. R., Heiss, C., & Azadi, P. (2023). Acetylation in ionic liquids dramatically increases yield in the glycosyl composition and linkage analysis of insoluble and acidic polysaccharides. *Analytical Chemistry*, *95*(34), 12851-12858.

Brennan, M., McLean, J. P., Altaner, C. M., Ralph, J., & Harris, P. J. (2012). Cellulose microfibril angles and cell-wall polymers in different wood types of *Pinus radiata*. *Cellulose*, *19*, 1385-1404.

Bunzel, M., Ralph, J., Marita, J. M., Hatfield, R. D., & Steinhart, H. (2001). Diferulates as structural components in soluble and insoluble cereal dietary fibre. *Journal of the Science of Food and Agriculture*, *81*(7), 653-660.

Callaway, J. (2004). Hempseed as a nutritional resource: An overview. *Euphytica*, *140*, 65-72.

Carpita, N. C., & Gibeaut, D. M. (1993). Structural models of primary cell walls in flowering plants: Consistency of molecular structure with the physical properties of the walls during growth. *The Plant Journal*, *3*(1), 1-30.

Chau, C.-F., Wang, Y. T., & Wen, Y. L. (2007). Different micronization methods significantly improve the functionality of carrot insoluble fibre. *Food Chemistry*, *100*(4), 1402-1408.

Chau, C. F., Wen, Y. L., & Wang, Y. T. (2006). Improvement of the functionality of a potential fruit insoluble fibre by micron technology. *International Journal of Food Science & Technology*, *41*(9), 1054-1060.

Chawla, R., & Patil, G. (2010). Soluble dietary fiber. *Comprehensive Reviews in Food Science and Food Safety*, *9*(2), 178-196.

Chio, C., Sain, M., & Qin, W. (2019). Lignin utilization: A review of lignin depolymerization from various aspects. *Renewable and Sustainable Energy Reviews*, *107*, 232-249.

790 Collins, H. M., Burton, R. A., Topping, D. L., Liao, M. L., Bacic, A., & Fincher, G. B. (2010). Variability in fine
791 structures of noncellulosic cell wall polysaccharides from cereal grains: potential importance in
792 human health and nutrition. *Cereal Chemistry*, *87*(4), 272-282.
793 Corradini, C., Cavazza, A., & Bignardi, C. (2012). High-performance anion-exchange chromatography
794 coupled with pulsed electrochemical detection as a powerful tool to evaluate carbohydrates of
795 food interest: principles and applications. *International Journal of Carbohydrate Chemistry*, *2012*.
796 Cosgrove, D. J. (2018). Diffuse growth of plant cell walls. *Plant Physiology*, *176*(1), 16-27.
797 de Carvalho, D. M., Martínez-Abad, A., Evtuguin, D. V., Colodette, J. L., Lindström, M. E., Vilaplana, F., &
798 Sevastyanova, O. (2017). Isolation and characterization of acetylated glucuronoarabinoxylan from
799 sugarcane bagasse and straw. *Carbohydrate Polymers*, *156*, 223-234.
800 De Ruiter, G. A., Schols, H. A., Voragen, A. G., & Rombouts, F. M. (1992). Carbohydrate analysis of water-
801 soluble uronic acid-containing polysaccharides with high-performance anion-exchange
802 chromatography using methanolysis combined with TFA hydrolysis is superior to four other
803 methods. *Analytical Biochemistry*, *207*(1), 176-185.
804 Den Besten, G., Van Eunen, K., Groen, A. K., Venema, K., Reijngoud, D.-J., & Bakker, B. M. (2013). The role
805 of short-chain fatty acids in the interplay between diet, gut microbiota, and host energy
806 metabolism. *Journal of Lipid Research*, *54*(9), 2325-2340.
807 Dodd, D., Mackie, R. I., & Cann, I. K. (2011). Xylan degradation, a metabolic property shared by rumen and
808 human colonic Bacteroidetes. *Molecular Microbiology*, *79*(2), 292-304.
809 Ertaş, N., & Aslan, M. (2020). Antioxidant and physicochemical properties of cookies containing raw and
810 roasted hemp flour. *Acta Scientiarum Polonorum Technologia Alimentaria*, *19*(2), 177-184.
811 Falk, H., & Stanek, M. (1997). Zweidimensionale 1 H und 13 C-NMR-Spektroskopie und die strukturellen
812 aspekte von amylose und amylopektin. *Monatshefte für Chemie/Chemical Monthly*, *128*, 777-784.
813 Föste, M., Verheyen, C., Jekle, M., & Becker, T. (2020). Fibres of milling and fruit processing by-products in
814 gluten-free bread making: A review of hydration properties, dough formation and quality-
815 improving strategies. *Food Chemistry*, *306*, 125451.
816 Fukushima, R. S., & Kerley, M. S. (2011). Use of lignin extracted from different plant sources as standards
817 in the spectrophotometric acetyl bromide lignin method. *Journal of Agricultural and Food*
818 *Chemistry*, *59*(8), 3505-3509.
819 Gebruers, K., Dornez, E., Boros, D., Dynkowska, W., Bedő, Z., Rakszegi, M., Delcour, J. A., & Courtin, C. M.
820 (2008). Variation in the content of dietary fiber and components thereof in wheats in the
821 HEALTHGRAIN diversity screen. *Journal of Agricultural and Food Chemistry*, *56*(21), 9740-9749.
822 Golovchenko, V. V., Khlopin, V. A., Patova, O. A., Vityazev, F. V., Dmitrenok, A. S., & Shashkov, A. S. (2024).
823 Structural characterization of arabinogalactan-II and pectin from *Urtica cannabina*. *Carbohydrate*
824 *Polymers*, 122868.
825 Hamauzu, Y., & Mizuno, Y. (2011). Non-extractable procyanidins and lignin are important factors in the bile
826 acid binding and radical scavenging properties of cell wall material in some fruits. *Plant Foods for*
827 *Human Nutrition*, *66*, 70-77.
828 Holscher, H. D. (2017). Dietary fiber and prebiotics and the gastrointestinal microbiota. *Gut Microbes*, *8*(2),
829 172-184.
830 House, J. D., Neufeld, J., & Leson, G. (2010). Evaluating the quality of protein from hemp seed (*Cannabis*
831 *sativa* L.) products through the use of the protein digestibility-corrected amino acid score method.
832 *Journal of Agricultural and Food Chemistry*, *58*(22), 11801-11807.
833 Joseleau, J.-P., & Pérez, S. (2016). The plant cell walls: complex polysaccharide nano-composites. In:
834 Glycopedia.
835 Joyce, G. E., Kagan, I. A., Flythe, M. D., Davis, B. E., & Schendel, R. R. (2023). Profiling of cool-season forage
836 arabinoxylans via a validated HPAEC-PAD method. *Frontiers in Plant Science*, *14*, 1116995.

Julakanti, S., Charles, A. P. R., Syed, R., Bullock, F., & Wu, Y. (2023). Hempseed polysaccharide (*Cannabis sativa* L.): Physicochemical characterization and comparison with flaxseed polysaccharide. *Food Hydrocolloids*, *143*, 108900.

Kale, M., Pai, D., Hamaker, B., & Campanella, O. (2011). Incorporation of fibers in foods: A food engineering challenge. Food Engineering Interfaces,

Keller, J., Marmit, S. P., & Bunzel, M. (2022). Structural characterization of dietary fiber from different lupin species (*Lupinus* sp.). *Journal of Agricultural and Food Chemistry*, *70*(27), 8430-8440.

Kim, H., & Ralph, J. (2014). A gel-state 2D-NMR method for plant cell wall profiling and analysis: A model study with the amorphous cellulose and xylan from ball-milled cotton linters. *Rsc Advances*, *4*(15), 7549-7560.

Kim, H., Ralph, J., & Akiyama, T. (2008). Solution-state 2D NMR of ball-milled plant cell wall gels in DMSO-*d*6. *BioEnergy Research*, *1*, 56-66.

Kitamura, M., Kiba, Y., Suzuki, R., Tomida, N., Uwaya, A., Isami, F., & Deng, S. (2020). Cannabidiol content and in vitro biological activities of commercial cannabidiol oils and hemp seed oils. *Medicines*, *7*(9), 57.

Korus, J., Witczak, M., Ziobro, R., & Juszczak, L. (2017). Hemp (*Cannabis sativa* subsp. sativa) flour and protein preparation as natural nutrients and structure forming agents in starch based gluten-free bread. *LWT*, *84*, 143-150.

Kromhout, D., Bosschieter, E., & Coulander, C. D. L. (1982). Dietary fibre and 10-year mortality from coronary heart disease, cancer, and all causes: The Zutphen Study. *The Lancet*, *320*(8297), 518-522.

Lacayo, C. I., Hwang, M. S., Ding, S.-Y., & Thelen, M. P. (2013). Lignin depletion enhances the digestibility of cellulose in cultured xylem cells. *PLoS One*, *8*(7), e68266.

Landucci, L., Smith, R. A., Liu, S., Karlen, S. D., & Ralph, J. (2020). Eudicot nutshells: Cell-wall composition and biofuel feedstock potential. *Energy & Fuels*, *34*(12), 16274-16283.

Leonard, W., Zhang, P., Ying, D., & Fang, Z. (2020). Hempseed in food industry: Nutritional value, health benefits, and industrial applications. *Comprehensive Reviews in Food Science and Food Safety*, *19*(1), 282-308.

Leonard, W., Zhang, P., Ying, D., Nie, S., Liu, S., & Fang, Z. (2022). Post-extrusion physical properties, techno-functionality and microbiota-modulating potential of hempseed (*Cannabis sativa* L.) hull fiber. *Food Hydrocolloids*, *131*, 107836.

Liu, D., Tang, W., Yin, J.-Y., Nie, S.-P., & Xie, M.-Y. (2021). Monosaccharide composition analysis of polysaccharides from natural sources: Hydrolysis condition and detection method development. *Food Hydrocolloids*, *116*, 106641.

Liu, J., Willför, S., & Xu, C. (2015). A review of bioactive plant polysaccharides: Biological activities, functionalization, and biomedical applications. *Bioactive Carbohydrates and Dietary Fibre*, *5*(1), 31-61.

Liu, Q., Luo, L., & Zheng, L. (2018). Lignins: Biosynthesis and biological functions in plants. *International Journal of Molecular Sciences*, *19*(2), 335.

Lucyszyn, N., Lubambo, A. F., Ono, L., Jó, T. A., De Souza, C. F., & Sierakowski, M. R. (2011). Chemical, physico-chemical and cytotoxicity characterisation of xyloglucan from *Guibourtia hymenifolia* (Moric.) J. Leonard seeds. *Food Hydrocolloids*, *25*(5), 1242-1250.

Luo, X., Wang, Q., Fang, D., Zhuang, W., Chen, C., Jiang, W., & Zheng, Y. (2018). Modification of insoluble dietary fibers from bamboo shoot shell: Structural characterization and functional properties. *International Journal of Biological Macromolecules*, *120*, 1461-1467.

Ma, M., & Mu, T. (2016). Modification of deoiled cumin dietary fiber with laccase and cellulase under high hydrostatic pressure. *Carbohydrate Polymers*, *136*, 87-94.

884 Mansfield, S. D., Kim, H., Lu, F., & Ralph, J. (2012). Whole plant cell wall characterization using solution-
885 state 2D NMR. *Nature Protocols*, *7*(9), 1579-1589.
886 Martínez, V., Mitjans, M., & Pilar Vinardell, M. (2012). Pharmacological applications of lignins and lignins
887 related compounds: An overview. *Current Organic Chemistry*, *16*(16), 1863-1870.
888 Merlino, M., Tripodi, G., Cincotta, F., Prestia, O., Miller, A., Gattuso, A., Verzera, A., & Condurso, C. (2022).
889 Technological, nutritional, and sensory characteristics of gnocchi enriched with hemp seed flour.
890 *Foods*, *11*(18), 2783.
891 Miao, W., Li, N., & Wu, J.-L. (2022). Food polysaccharides utilization via in vitro fermentation: Microbiota,
892 structure, and function. *Current Opinion in Food Science*, 100911.
893 Mikulec, A., Kowalski, S., Sabat, R., Skoczylas, Ł., Tabaszewska, M., & Wywrocka-Gurgul, A. (2019). Hemp
894 flour as a valuable component for enriching physicochemical and antioxidant properties of wheat
895 bread. *LWT*, *102*, 164-172.
896 Navarro, D. M., Abelilla, J. J., & Stein, H. H. (2019). Structures and characteristics of carbohydrates in diets
897 fed to pigs: A review. *Journal of Animal Science and Biotechnology*, *10*(1), 1-17.
898 Norajit, K., Gu, B.-J., & Ryu, G.-H. (2011). Effects of the addition of hemp powder on the physicochemical
899 properties and energy bar qualities of extruded rice. *Food Chemistry*, *129*(4), 1919-1925.
900 Nystrom, L., Lampi, A.-M., Andersson, A. A., Kamal-Eldin, A., Gebruers, K., Courtin, C. M., Delcour, J. A., Li,
901 L., Ward, J. L., & Fras, A. (2008). Phytochemicals and dietary fiber components in rye varieties in
902 the HEALTHGRAIN diversity screen. *Journal of Agricultural and Food Chemistry*, *56*(21), 9758-9766.
903 O'Neill, M. A., Ishii, T., Albersheim, P., & Darvill, A. G. (2004). Rhamnogalacturonan II: Structure and
904 function of a borate cross-linked cell wall pectic polysaccharide. *Annual Review of Plant Biology*,
905 *55*, 109-139.
906 Pettolino, F. A., Walsh, C., Fincher, G. B., & Bacic, A. (2012). Determining the polysaccharide composition
907 of plant cell walls. *Nature Protocols*, *7*(9), 1590-1607.
908 Pettolino, F. A., Yulia, D., Bacic, A., & Llewellyn, D. J. (2022). Polysaccharide composition during cotton seed
909 fibre development: Temporal differences between species and in different seasons. *Journal of*
910 *Cotton Research*, *5*(1), 27.
911 Pojić, M., Dapčević Hadnađev, T., Hadnađev, M., Rakita, S., & Brlek, T. (2015). Bread supplementation with
912 hemp seed cake: A by-product of hemp oil processing. *Journal of Food Quality*, *38*(6), 431-440.
913 Rencoret, J., Kim, H., Evaristo, A. B., Gutiérrez, A., Ralph, J., & Del Río, J. C. (2018). Variability in lignin
914 composition and structure in cell walls of different parts of macaúba (*Acrocomia aculeata*) palm
915 fruit. *Journal of Agricultural and Food Chemistry*, *66*(1), 138-153.
916 Ridley, B. L., O'Neill, M. A., & Mohnen, D. (2001). Pectins: Structure, biosynthesis, and oligogalacturonide-
917 related signaling. *Phytochemistry*, *57*(6), 929-967.
918 Robin, F., Schuchmann, H. P., & Palzer, S. (2012). Dietary fiber in extruded cereals: Limitations and
919 opportunities. *Trends in Food Science & Technology*, *28*(1), 23-32.
920 Rodriguez-Leyva, D., & Pierce, G. N. (2010). The cardiac and haemostatic effects of dietary hempseed.
921 *Nutrition & Metabolism*, *7*(1), 1-9.
922 Scheller, H. V., & Ulvskov, P. (2010). Hemicelluloses. *Annual Review of Plant Biology*, *61*, 263-289.
923 Schendel, R. R., Becker, A., Tyl, C. E., & Bunzel, M. (2015). Isolation and characterization of feruloylated
924 arabinoxylan oligosaccharides from the perennial cereal grain intermediate wheat grass
925 (*Thinopyrum intermedium*). *Carbohydrate Research*, *407*, 16-25.
926 Schultz, C. J., Lim, W. L., Khor, S. F., Neumann, K. A., Schulz, J. M., Ansari, O., Skewes, M. A., & Burton, R. A.
927 (2020). Consumer and health-related traits of seed from selected commercial and breeding lines
928 of industrial hemp, *Cannabis sativa* L. *Journal of Agriculture and Food Research*, *2*, 100025.
929 Sciacca, F., Virzì, N., Pecchioni, N., Melilli, M. G., Buzzanca, C., Bonacci, S., & Di Stefano, V. (2023).
930 Functional End-Use of Hemp Seed Waste: Technological, Qualitative, Nutritional, and Sensorial
931 Characterization of Fortified Bread. *Sustainability*, *15*(17), 12899.

Sedlmeyer, F. (2011). Xylan as by-product of biorefineries: Characteristics and potential use for food applications. *Food Hydrocolloids*, *25*(8), 1891-1898.

Shakhmatov, E. G., Belyy, V. A., & Makarova, E. N. (2017). Structural characteristics of water-soluble polysaccharides from Norway spruce (*Picea abies*). *Carbohydrate Polymers*, *175*, 699-711.

Shewry, P. R., Piironen, V., Lampi, A.-M., Nystrom, L., Li, L., Rakszegi, M., Fras, A., Boros, D., Gebruers, K., & Courtin, C. M. (2008). Phytochemical and fiber components in oat varieties in the HEALTHGRAIN diversity screen. *Journal of Agricultural and Food chemistry*, *56*(21), 9777-9784.

Singh, S., Singh, G., & Arya, S. K. (2018). Mannans: An overview of properties and application in food products. *International Journal of Biological Macromolecules*, *119*, 79-95.

Slavin, J. L. (2005). Dietary fiber and body weight. *Nutrition*, *21*(3), 411-418.

Sticklen, M. B. (2008). Plant genetic engineering for biofuel production: Towards affordable cellulosic ethanol. *Nature Reviews Genetics*, *9*(6), 433-443.

Teleman, A., Lundqvist, J., Tjerneld, F., Stålbrand, H., & Dahlman, O. (2000). Characterization of acetylated 4-*O*-methylglucuronoxylan isolated from aspen employing 1H and 13C NMR spectroscopy. *Carbohydrate Research*, *329*(4), 807-815.

Unda, F., Kim, H., Hefer, C., Ralph, J., & Mansfield, S. D. (2017). Altering carbon allocation in hybrid poplar (*Populus alba*× *grandidentata*) impacts cell wall growth and development. *Plant Biotechnology Journal*, *15*(7), 865-878.

Vonapartis, E., Aubin, M.-P., Seguin, P., Mustafa, A. F., & Charron, J.-B. (2015). Seed composition of ten industrial hemp cultivars approved for production in Canada. *Journal of Food Composition and Analysis*, *39*, 8-12.

Wang, D., Wang, Q., Sun, Y., Qing, Z., Zhang, J., & Chen, Q. (2023). Effect of insoluble dietary fiber extracted from feijoa (*Acca sellowiana* (O. Berg) Burret.) supplementation on physicochemical and functional properties of wheat bread. *Foods*, *12*(10), 2019.

Wang, T., Park, Y. B., Cosgrove, D. J., & Hong, M. (2015). Cellulose-pectin spatial contacts are inherent to never-dried Arabidopsis primary cell walls: Evidence from solid-state nuclear magnetic resonance. *Plant Physiology*, *168*(3), 871-884.

Wefers, D., & Bunzel, M. (2015). Characterization of dietary fiber polysaccharides from dehulled common buckwheat (*Fagopyrum esculentum*) seeds. *Cereal Chemistry*, *92*(6), 598-603.

Wefers, D., & Bunzel, M. (2016). Arabinan and galactan oligosaccharide profiling by high-performance anion-exchange chromatography with pulsed amperometric detection (HPAEC-PAD). *Journal of Agricultural and Food Chemistry*, *64*(22), 4656-4664.

Wefers, D., Gmeiner, B. M., Tyl, C. E., & Bunzel, M. (2015). Characterization of diferuloylated pectic polysaccharides from quinoa (*Chenopodium quinoa* WILLD.). *Phytochemistry*, *116*, 320-328.

Wefers, D., Tyl, C. E., & Bunzel, M. (2015). Neutral pectin side chains of amaranth (*Amaranthus hypochondriacus*) contain long, partially branched arabinans and short galactans, both with terminal arabinopyranoses. *Journal of Agricultural and Food Chemistry*, *63*(2), 707-715.

Wen, Z.-S., Xue, R., Du, M., Tang, Z., Xiang, X.-W., Zheng, B., & Qu, Y.-L. (2019). Hemp seed polysaccharides protect intestinal epithelial cells from hydrogen peroxide-induced oxidative stress. *International Journal of Biological Macromolecules*, *135*, 203-211.

Woomer, J., Schendel, R., Lovely, J., Vijayakumar, P. P., & Adedeji, A. A. (2023). Value-added application of bourbon spent grain and proso millet for high-fiber extruded product. *Journal of the ASABE*, *66*(5), 1019-1032.

Xue, R., Du, M., Zhou, T.-Y., Ai, W.-Z., Zhang, Z.-S., Xiang, X.-W., Zhou, Y.-F., & Wen, Z.-S. (2020). Polysaccharides from hemp seed protect against cyclophosphamide-induced intestinal oxidative damage via Nrf2-Keap1 signaling pathway in mice. *Oxidative Medicine and Cellular Longevity*, *2020*.

Yu, C., Ahmadi, S., Shen, S., Wu, D., Xiao, H., Ding, T., Liu, D., Ye, X., & Chen, S. (2022). Structure and fermentation characteristics of five polysaccharides sequentially extracted from sugar beet pulp by different methods. *Food Hydrocolloids*, *126*, 107462.

Zając, M., Guzik, P., Kulawik, P., Tkaczewska, J., Florkiewicz, A., & Migdał, W. (2019). The quality of pork loaves with the addition of hemp seeds, de-hulled hemp seeds, hemp protein and hemp flour. *LWT*, *105*, 190-199.